

Green Communications and Networking

October 31, 2011

Contents

- 1 Green Relay Techniques in Cellular Systems 1**
- 1.1 Introduction 2
- 1.2 Spectrum and Energy Efficiency Analysis of Relay-assisted Systems 6
 - 1.2.1 System Model 8
 - 1.2.2 Spectrum Efficiency Analysis 9
 - 1.2.3 Energy Efficiency Analysis 14
 - 1.2.4 Insights and discussions 21
- 1.3 H-ARQ Relaying and H²-ARQ Relaying 22
 - 1.3.1 H²-ARQ Relaying Strategy 23
 - 1.3.2 Performance Analysis 25
 - 1.3.3 Insights and Discussions 28
- 1.4 Energy Efficient RNs in Cellular Networks 30
 - 1.4.1 Cellular System and Power Model 32
 - 1.4.2 Optimization of RN Deployment 34

| | | |
|-------|---------------------------------------|----|
| 1.4.3 | Outdoor-to-Indoor Relaying | 38 |
| 1.5 | Conclusion and Future Works | 42 |

Chapter 1

Green Relay Techniques in Cellular Systems

Yinan Qi, Fabien Hélot, Muhammad Ali Imran and Rahim Tafazolli
University of Surrey, yinan.qi@surrey.ac.uk

There has been escalated demand for rapid, low-latency and high-rate communication of information at homes and business premises in the past decade. As the need for high speed access by end-users evolved, particularly fuelled by the widespread adoption of the wireless internet (smart phone), some standards such as High-Speed Downlink Packet Access (HSDPA) [1], 3rd Generation Partnership Project Long Term Evolution (3 GPP LTE) as well as its major enhancement LTE-Advanced for mobile phone networks [2, 3], and IEEE standard for mobile broadband wireless access, also known as “mobile Worldwide Interoperability for Microwave Access (WiMAX)” [4], have been proposed to provide high speed data transmission.

One of the main objectives of future wireless systems is to provide high data rate with a uniform coverage by adapting itself to multipath fading, path-loss and shadowing conditions. In the pursuit of finding schemes that will provide a solution to minimize these effects,

various granular and distributed network architectures based on relaying techniques are emerging. However, due to the increasing concern about the CO₂ contribution from the ICT (Information and Communications Technology) industry [5, 6], the future wireless systems should also be energy efficient to meet the increasing demand for flexible use of emerging green technologies, where relay is no doubt one of the strongest candidates.

This chapter analyzes the relaying technique at link and system levels from both spectrum efficiency (Se) and energy efficiency (EE) perspectives. A throughout investigation will be provided for a variety of approaches at the relay node (RN) to forward information including amplify-and-forward (AF), decoding-and-forward (DF), compress-and-forward (CF). Advanced relaying schemes, where the conventional relaying schemes are combined in a hybrid manner to adapt to the variations of the channel states, are introduced and investigated. Furthermore, the relaying techniques are combined with retransmission protocols for packet oriented communication systems and a study from spectrum and energy efficiency perspectives is presented. Finally, this chapter also addresses the challenge of designing and positioning RNs in a state-of-the-art wireless cellular system, namely LTE system, coupled with practical power consumption models.

The rest of the chapter is organized as follows: section 1 introduces the broad topic of relaying. In the next section, the analysis of a relay-assisted system is presented from the spectrum and energy efficiency perspectives. Relay is further combined with retransmission protocols and its performance is studied in section 3. The energy efficiency of relaying techniques in cellular networks is investigated in section 4 and the final section summarizes the findings of the chapter and identifies the potential future works.

1.1 Introduction

In recent years, many projects focusing on cooperative communications have been launched by the 7th Framework Programme of the European Commission, such as FIREWORKS (FlexIble RElay Wireless OFDM-based networks)[7] and ROCKET (Reconfigurable OFDMA-based Cooperative NetworKs Enabled by Agile SpecTrum Use) [8]. Recently, the “green”

potential of cooperative communication for improving the energy efficiency (EE) has drawn considerable attention towards this topic from both academia and industry. For instance, theoretical analysis of relaying technology from an EE point of view have been recently conducted in [9, 12]. Moreover, major research projects focusing on green communications, such as EU FP7 project EARTH (Energy Aware Radio and network tecHnologies) [13], have considered relay as one of their main research tracks.

The basic idea behind relaying is to use some radio nodes, called relays, in order to enable more spectrum and energy efficient communications. RNs can be specifically devoted network nodes or can be other user devices in the vicinity, as it is depicted in Figure (1.1). For instance in an urban environment, the direct source-destination link can be impaired because of buildings and with the help of a fixed or mobile RN, another independent link, i.e. source-RN-destination, can be established for improving the communication between the source and destination nodes. This link does not suffer from shadowing effect because it is obstacle free. There are two basic working modes for a relay system: full-duplex and half-duplex. In full-duplex mode, the relay is assumed to be able to transmit and receive simultaneously. Due to the large dynamic range between the incoming and outgoing signals through the same antenna elements, the full-duplex mode is regarded as difficult to implement in reality. In contrast, in half-duplex mode, the relay is assumed to work in a time-division manner, where it either receives or transmits at a given time and band instance. Compared with the full-duplex mode, the half-duplex mode is more practical. Therefore, we will focus here on the time-division half-duplex relay channel. The entire frame is separated into two phases: the relay-receive phase (phase 1) and the relay-transmit phase (phase 2). During the first phase, the source broadcasts to the relay and the destination. In phase 2, the source and the relay transmits to the destination simultaneously, as it is shown Figure 1.2). The duplexing ratio in percentage, denoted by α , represents the ratio of the duration of the first phase to the duration of the total transmission.

The relaying model was first introduced by van der Meulen [14], where a communication system with three nodes denoted as source (S), relay node (RN) and destination (D), respectively, was investigated. There are three links between these nodes and each link has an input/output pair. Cover and El Gamal have substantially developed the relaying model

and provided three basic relaying principles [15]:

1. Cooperation: If the relay receives a better signal than the destination, it is able to cooperate with the source by sending a signal that contains a perfect source signal to the destination.
2. Facilitation: If the relay sees a corrupted version of what the destination sees, the relay transmits constant signal which is known to the source and the destination to open the channel between the source and the destination.
3. Observation: Alternative information can be sent by the relay. This information does not comprise a perfect source signal, thus precluding pure cooperation, and is not constant, thus precluding simple facilitation. Instead, the relay forwards what it has observed to the destination.

While the optimal relaying strategy in wireless networks has not yet been fully understood, several relaying schemes developed based on the principles (especially for cooperation and observation) have been suggested in the literature. Among them, the simplest scheme is amplify-and-forward (AF) [16]- [19], in which the relay just forwards what it has received with a proper amplification gain. Another well developed scheme is decoded-and-forward (DF)[20]- [27], where the relay decodes, re-encodes and forwards the received signal to the destination. DF has shown improvement in terms of the achievable rate and outage behavior when the relay is close to the source, [20] and [27]- [28]. Both schemes share a common weakness: their performance is constrained by the quality of the source-relay link. If this link endures deep fading, for AF the relay will forward nothing but mostly its own noise, and for DF the relay will not be able to successfully decode and forwarding of erroneous messages will lead to error propagation at the destination. To cope with this problem, an effective solution for the case of a weak source-relay link based on the observation principle in Cover's paper [15] is to forward the relay's observation to the destination [29]- [31]. Instead of decoding, the relay quantizes the received signal, compresses the quantized version and forwards the compressed version to the destination. Studies on CF reveal that it outperforms DF when the relay is close to the destination, or generally speaking, the relay-destination link is very strong. The conventional forwarding mechanisms can be combined in a hybrid

fashion to avoid the shortcomings of the original ones. In [32] and [33], the hybrid AF/DF forwarding scheme is able to improve the considered system's frame error rate (FER). The hybrid approach has been further extended by taking CF into consideration in [29] and [34]. The proposed hybrid scheme avoids the shortcomings of AF and DF and exhibits remarkable improvement in outage performance. In wireless broadband networks, relay is being studied as a technology that offers the possibility to extend coverage and increase capacity as shown in figure (1.3), allowing more flexible and cost-effective deployment options [35]. The link between the donor base station (BS) and the RN is called backhaul link and the link between the RN and the user equipment (UE) is called access link as shown in figure (1.3).

Many standards have included relay as part of their study items as follows

1. IEEE 802.16j (16j Relay) [36],
2. IEEE 802.16m (Relay and Femtocell) [37],
3. 3GPP LTE-A (Rel-10 LTE-A Relay) [38].

Based on its functionalities, a number of different classifications exist for RNs. Relay is usually classified as inband relay when the same carrier frequency is used for the backhaul and access links and outband relay when different carrier frequencies are used for these links. Relay can also be categorized with respect to protocol layer functionalities. A Layer 1 RN, also known as repeater, simply pick up the donor BS signal, amplifies and forwards it into its own coverage area. In contrast with Layer 1 RN, a Layer 2 RN has medium access control (MAC) layer functionality, it can decode received signals and re-encode transmitted signals in order to achieve higher quality in the relay cell area. A Layer 3 RN would include functionalities like mobility management, session set-up and handover and as such acts as a full service BS. This type of relay adds more complexity to the implementation and increases further the delay. In 3GPP standardization [35], RNs are distinguished between Type 1 and Type 2. Type 1 relays are RNs operating on Layer 3, i.e. protocol layer up to Layer 3 for user data packets is available at the RN. Such Layer 3 RNs have all functions that a BS has, and they effectively create their own identity number (Cell-ID) and own synchronization and reference signals. Type 1 RNs are considered visible to the UEs, thus

being called as non-transparent RNs. In contrast, Type 2 RNs will not have their own Cell-ID. Consequently the UEs will not be able to distinguish between transmitted signals from the BSs and the RNs. Type 2 RNs operates in Layer 3 or Layer 2, depending on the particular solution/implementation and are transparent to UEs.

An important aspect of the design of spectrum and energy efficient relaying schemes requires an understanding of the measurable spectrum and energy metrics. The spectrum efficiency (SE) can be easily evaluated in terms of achievable rate with the metric bit/second/Hz (bps/Hz). It is important for us to adopt a well-defined and relevant performance metrics to quantify and assess the energy efficiency performance. To capture the energy consumption perspective in the analysis, we employ the energy consumption index bits to energy consumption ratio, defined as the total number of bits that were correctly delivered divided by the energy consumption during the observation period and measured in [bits/J]. The bits to energy consumption ratio metric focuses on the amount of bits spent per Joule and is hence an indicator of bit delivery energy efficiency. The inverse of the bits to energy consumption ratio, measured by Joule per bit, can also be used for evaluation purpose indicating how much energy is needed to convey one bit [39]. In this chapter, we use both to help the reader understand the energy efficiency problem from different perspectives.

1.2 Spectrum and Energy Efficiency Analysis of Relay-assisted Systems

In wireless networks, relaying techniques have been traditionally used to extend the coverage of communication systems. However, in recent years, other relaying schemes to assist in the communications between the source and destination via some cooperation protocols have emerged. By controlling medium access between the source and the relay coupled with appropriate modulation or coding strategies in such cooperative schemes, it has been found that the diversity gain of the system can be improved. In particular, three basic relaying schemes have been proposed including amplify-and-forward (AF), decode-and-forward (DF) and compress-and-forward (CF).

Among various cooperative protocols, AF is one of the basic modes and has attracted lots of attention in recent years due to its simplicity and low expenses. AF is especially suitable for systems with strict energy consumption constraints on RNs because no baseband processing is needed, thus the RF links can be saved and the energy consumption can be further reduced in addition to the saved baseband processing energy. Being a non-regenerative scheme, AF only allows RN to amplify and forward the received signals to the destination without any coding or decoding process. Laneman has, in his landmark paper [27], pointed out that AF is able to achieve second-order diversity in very high SNR regions. Another work indicated that the ergodic capacity of AF can be higher than that of DF with certain SNR settings [16]. In particular, when the source-relay link is statistically worse than the other two links, AF is more spectrum efficient than DF.

Other two basic relaying schemes have been introduced in the classic work of Cover and El Gamal [15]. One is DF, where the RN decodes the received message completely, re-encodes the message and fully or only partially forwards the decoded message to the destination. It has been proved that DF is able to achieve the capacity of the degraded relay channel. The information-theoretical analysis of the outage behavior in Laneman's work [25] indicates that fixed decode-and-forward (FDF), where the RN always forwards the decoded message even when the decoding is unsuccessful, does not achieve diversity. In contrast, selective DF in which RN keeps silent when it is not able to decode the message achieves full cooperative diversity in high SNR regions. Another basic relaying scheme is CF [29]. In CF, the operation of RN is quite different. Instead of decoding, RN compresses the received signal and transmits the compressed version to the destination. As a result, at the destination, the signal received from the source during phase 1 will serve as side information to reconstruct RN's observation of the signal from the source. Then the destination tries to decode the message by joint processing of the received signal and the reconstructed observation of the RN. To help the readers better understand this point, we can just assume an extreme case where the RN and the destination can fully share their observations without any distortion. In such a case, the RN and destination can enjoy full receive diversity. In contrast to DF, which normally exhibits superior performance when the RN is close to the source, CF is desired under the condition of a weak source to RN link and a strong RN to destination link.

However, the wireless channels suffer from fading occasionally. Even when the RN is close to the source or destination, the instantaneous SNRs of the links are not always apposite for one single relaying scheme. For instance, the RN cannot successfully decode every block no matter how close it is to the source. Thus DF cannot be guaranteed to be successful all the time. We need to develop a flexible relay system which is able to adapt itself to the dynamics of the channel. Inspired by this idea, advanced relaying schemes were proposed in [29] and [32]- [34], where the conventional forwarding mechanisms can be combined in a hybrid fashion to avoid the shortcomings of the original ones. There is another hybrid structure introduced in [40], where the multilevel coding concept is incorporated. This structure exploits the fact that bit-error-rates (BERs) of different coding levels exhibit considerable difference and the authors propose to use DF in the levels where decoding is more likely to be successful, and in the mean time CF in the levels where the error probability of decoding increases significantly. However, this scheme is just a preliminary one and therefore not included in this chapter.

1.2.1 System Model

Consider a relay-assisted system where the source transmits a W bit message $w \in \{1, \dots, 2^W\}$ to the destination. During the first phase, the source encodes the message into αn symbols $x^1(w)[1], \dots, x^1(w)[\alpha n]$ and broadcasts to the RN and the destination. The received signals at the RN and the destination are given by

$$\begin{aligned} y_r[i] &= \frac{c_1}{\sqrt{K_t d_1^\zeta}} x^1(w)[i] + z_r[i], \\ y_d^1[i] &= \frac{c_0}{\sqrt{K_t d_0^\zeta}} x^1(w)[i] + z_d[i], \end{aligned} \quad (1.1)$$

respectively, where c_0 and c_1 are the channel gains of the S-D and S-RN links, modelled by circularly symmetric complex Gaussian distribution with zeros means and unit variances, d_0 and d_1 are distances of the S-D and S-RN links, respectively, ζ is the path-loss exponent, K_t is a constant indicating the physical characteristics of the link and the power amplifier as in [9] and [41], and z_r and z_d are the additive noise modelled by circularly symmetric complex

Gaussian distribution with zeros means. The superscript indicates phase when necessary. The encoded message should be subject to the power constraint

$$\frac{1}{\alpha n} \sum_{i=1}^{\alpha n} |x^1[i]|^2 \leq P_s, \quad (1.2)$$

During phase 2, the RN transmits $(1 - \alpha)n$ encoded symbols $x_r[1], \dots, x_r[(1 - \alpha)n]$; while at the same time the source transmits symbols $x^2(w)[1], \dots, x^2(w)[(1 - \alpha)n]$. The signal received by the destination is

$$y_d^2[i] = \frac{c_0}{\sqrt{K_t d_0^{\zeta/2}}} x^2(w)[i] + \frac{c_2}{\sqrt{K_t d_2^{\zeta/2}}} x_r[i] + z_d[i], \quad (1.3)$$

where d_2 and c_2 are the distance and channel gain of the RN-D link, respectively and c_2 follow the same distribution as c_0 and c_1 . It should be noted that we did not specify the operation of the RN because it is depending on the employed relaying schemes.

1.2.2 Spectrum Efficiency Analysis

With a well defined signal model, we can study the spectrum efficiency of the relay-assisted systems in terms of achievable rate. We also analyze their outage probability which indicates the unsuccessful reception at the destination and will be used in the energy efficiency analysis. Starting from non-hybrid relaying schemes, the analysis will be further developed to hybrid ones.

AF: In AF, the duplexing ratio is fixed at 0.5 and we assume that the source transmits exactly the same symbols during two phases. The signal transmitted by the RN is

$$\begin{aligned} x_r[i] &= \beta y_r[i] \\ &= \beta \left(\frac{c_1}{\sqrt{K_t d_1^{\zeta/2}}} x^1(w)[i] + z_r[i] \right), \end{aligned} \quad (1.4)$$

where β is the amplification gain and subject to the power constraint

$$\beta \leq \sqrt{\frac{P_r}{\frac{|c_1|^2 P_s}{K_t d_1^\zeta} + N_0 B}}. \quad (1.5)$$

Here N_0 is the noise power spectral density and B is the bandwidth. The received signal at the destination can be given by

$$y_d^2[i] = \frac{c_0}{\sqrt{K_t d_0^{\zeta/2}}} x^2(w)[i] + \frac{c_2}{\sqrt{K_t d_2^{\zeta/2}}} \beta y_r[i] + z_d[i] \quad (1.6)$$

$$= \frac{c_0}{\sqrt{K_t d_0^{\zeta/2}}} x^2(w)[i] + \frac{c_2}{\sqrt{K_t d_2^{\zeta/2}}} \beta \left(\frac{c_1}{\sqrt{K_t d_1^{\zeta/2}}} x^1(w)[i] + z_r[i] \right) + z_d[i] \quad (1.7)$$

$$= \left(\frac{c_0}{\sqrt{K_t d_0^{\zeta/2}}} + \beta \frac{c_1 c_2}{K_t (d_1 d_2)^{\zeta/2}} \right) x(w)[i] + \left(\beta \frac{c_2}{\sqrt{K_t d_2^{\zeta/2}}} z_r[i] + z_d[i] \right),$$

where $x(w)[i] = x^1(w)[i] = x^2(w)[i]$ for $1 \leq i \leq n/2$. The achievable rate R_{AF} can be derived as in [10]. The closed-form expression for R_{AF} is difficult to calculate since carrier phase synchronization is not assumed here but the trivial upper bound has been derived in [42] as

$$\bar{R}_{AF} = B \log_2 \left(1 + \frac{|c_0|^2 P_s}{N_0 B K_t d_0^\zeta} + \frac{P_s \left(\frac{\beta^2 |c_1 c_2|^2}{K_t^2 (d_1 d_2)^\zeta} + \frac{|c_0|^2}{K_t d_0^\zeta} \right)}{N_0 B \left(1 + \frac{\beta^2 |c_2|^2}{K_t d_2^\zeta} \right)} \right). \quad (1.8)$$

\bar{R}_{AF} is a function of amplification gain β and can be rewritten as

$$\bar{R}_{AF} = B \log_2 \left(1 + \frac{|c_0|^2 P_s}{N_0 B K_t d_0^\zeta} + \frac{|c_1|^2 P_s}{N_0 B K_t d_1^\zeta} + \frac{|c_1|^2 P_s \left(\frac{|c_0|^2 d_1^\zeta}{|c_1|^2 d_0^\zeta} - 1 \right)}{N_0 B K_t d_1^\zeta \left(1 + \frac{\beta^2 |c_2|^2}{K_t d_2^\zeta} \right)} \right). \quad (1.9)$$

Apparently, in order to maximize \bar{R}_{AF} and taking the constraint (1.5) into account, β should be chosen as

$$\beta = \begin{cases} \sqrt{\frac{P_r}{\frac{|c_1|^2 P_s}{K_t d_1^\zeta} + N_0 B}} & \text{if } |c_0|^2 d_1^\zeta \leq |c_1|^2 d_0^\zeta \\ 0 & \text{otherwise.} \end{cases} \quad (1.10)$$

It reveals the fact that the RN is not necessary to always amplify and forward its reception.

It only forwards when the S-RN link is of higher quality than a certain threshold. This makes sense because once the S-RN link is weak, a large part of the received signal of the RN is comprised of noise and nothing by noise is forwarded to the destination if the RN insisting on transmitting. In such a case, the final decoding is not benefiting from the RN's forwarding but rather being affected adversely. Thus we can draw the conclusion that if the RN cannot help, it should just stop doing so.

DF : As we mentioned before, DF is more complicated than AF in the sense that the RN needs to decode, re-encode and forward the received message. The received message at destination during phase 2 is

$$y_d^2[i] = \frac{c_0}{\sqrt{K_t d_0^{\zeta/2}}} x^2(w)[i] + \frac{c_2}{\sqrt{K_t d_2^{\zeta/2}}} x_r(w)[i] + z_d[i], \quad (1.11)$$

where $1 \leq i \leq (1 - \alpha)n$. The encoding at the RN and the destination can be carefully designed to form a MISO code to enjoy the transmit diversity. The achievable rate of DF can be given as [28]

$$R_{DF} = \min\{R^1, R^2\}, \quad (1.12)$$

where

$$\begin{aligned} R^1 &= \alpha B \log_2 \left(1 + \frac{|c_1|^2 P_s}{N_0 B K_t d_1^\zeta} \right), \\ R^2 &= \alpha B \log_2 \left(1 + \frac{|c_0|^2 P_s}{N_0 B K_t d_0^\zeta} \right) + (1 - \alpha) B \log_2 \left(1 + \frac{|c_0|^2 P_s}{N_0 B K_t d_0^\zeta} + \frac{|c_2|^2 P_r}{N_0 B K_t d_2^\zeta} \right). \end{aligned} \quad (1.13)$$

The first term R^1 implies that the RN has to successfully decode the message before forwarding it.

CF : CF is even more complicated than DF. In instead of amplifying or decoding, the RN tries to help the destination by forwarding its own observation y_r , which requires a source coding scheme for the continuous y_r . During the first phase, the signals received by the RN and the destination both originate from the same source and contain a common term $x^1(w)$. Thus these two signals are correlated and this fact provides the possibility of transmitting the observation of the RN at a reduced rate, i.e. y_r can be compressed.

Wyner-Ziv coding is an efficient method for compressing correlated continuous sources which are separately located [43]- [44]. It is an extension of the work of Slepian and Wolf in [45], where discrete distributed source coding is investigated. Although the details of distributed coding might help the readers better understand the compression mechanism in CF, it is out of the scope of this book and interested readers can refer to [43]- [44] for in-depth knowledge. It has been pointed out that nested multi-dimensional lattice code can be used for Wyner-Ziv coding [46]- [47]. However, nested multi-dimensional lattice code requires high complexity and is not feasible for practical implementation. A more feasible two step structure consists of a quantizer and a Slepian Wolf encoder, i.e. compressor is proposed in [48]. Firstly, the quantizer converts continuous reception into discrete bin index. Secondly, the Slepian Wolf encoder compresses the bin index.

Coming back to our system, at the end of the first phase, the RN quantizes the received signal y_r into some intermediate bin index u , which is then compressed into index v by the Slepian Wolf encoder. The index v is encoded into symbols $x_r(v)[1], \dots, x_r(v)[(1 - \alpha)n]$ and forwarded during the second phase. Meanwhile, the source transmits $x^2(w)$ independent with $x_r(v)$. In this regard, a multiple access channel is formed and the received signal at the destination is

$$y_d^2[i] = \frac{c_0}{\sqrt{K_t d_0^{\zeta/2}}} x^2(w)[i] + \frac{c_2}{\sqrt{K_t d_2^{\zeta/2}}} x_r(v)[i] + z_d[i], \quad (1.14)$$

The destination starts from decoding the Slepian Wolf coded bin index v by treating $x^2(w)$ as noise. The destination then, with the help of the side information y_d^2 , decompresses v and uses the decompressed u to reconstruct the observation of the RN, denoted as \hat{y}_r . The destination then subtracts $x_r(v)$ from y_d^2 to get

$$\bar{y}_d^2[i] = y_d^2[i] - \frac{c_2}{\sqrt{K_t d_2^{\zeta/2}}} x_r(v)[i]. \quad (1.15)$$

Then the destination performs final decoding by joint processing of y_d^2, \bar{y}_d^2 and the estimated \hat{y}_r . The achievable rate of CF is derived in [42] as

$$R_{CF} = \alpha B \log_2 \left(1 + \frac{|c_0|^2 P_s}{N_0 B K_t d_0^\zeta} + \frac{|c_1|^2 P_s}{(N_0 B + \sigma_U^2) K_t d_1^\zeta} \right) + (1 - \alpha) B \log_2 \left(1 + \frac{|c_0|^2 P_s}{N_0 B K_t d_0^\zeta} \right), \quad (1.16)$$

where σ_U^2 is the compression noise variance. In order to maximize the achievable rate, the compression noise should be minimized as follows. During phase 2, the destination can successfully decode v if

$$R_0 \leq I(X_r; Y_d^2) = \log_2 \left(1 + \frac{\frac{|c_2|^2 P_r}{K_t d_2^c}}{N_0 B + \frac{|c_0|^2 P_s}{K_t d_0^c}} \right), \quad (1.17)$$

where R_0 is transmission rate of the compressed information. On the other side, the minimum transmission rate for the compressed signal, such that it can be recovered with the smallest distortion, is given in [28] as,

$$H(Y_r + U|Y_d^1) - H(Y_r + U|Y_r) = \log_2 \left(\frac{\frac{|c_1|^2 P_s N_0 B}{K_t d_0^c}}{N_0 B + \frac{|c_0|^2 P_s}{K_t d_0^c}} + N_0 B + \sigma_U^2 \right) - \log_2(\sigma_U^2) \quad (1.18)$$

where U is an auxiliary random variable following circularly symmetric complex Gaussian distribution with zero mean and variance σ_U^2 . In order to satisfy both constraints, we have

$$(1 - \alpha)R_0 \leq \alpha \left(H(Y_r + U|Y_d^1) - H(Y_r + U|Y_r) \right), \quad (1.19)$$

leading to

$$\sigma_U^2 \geq \frac{\frac{|c_1|^2 P_s N_0 B}{K_t d_0^c} + N_0 B \left(N_0 B + \frac{|c_0|^2 P_s}{K_t d_0^c} \right)}{\left(2^{\frac{(1-\alpha)R_0}{\alpha B}} - 1 \right) \left(N_0 B + \frac{|c_1|^2 P_s}{K_t d_1^c} \right)}, \quad (1.20)$$

where σ_U^2 can be minimized when equal holds.

Hybrid Schemes : In a fading environment, the instantaneous SNRs always change in a wide range. Thus no single relaying scheme is able to outperform others all the time. Other than AF, DF and CF, some advanced hybrid relaying schemes, where the conventional forwarding mechanisms are combined in a hybrid fashion, will be addressed. These hybrid schemes are able to adapt themselves to the variations of the time-varying channel and achieve either transmit or receive diversity depending on the current channel state. This sub-section will investigate these hybrid schemes. We focus on DF/CF hybrid relaying and all the derivations can be easily extended to other hybrid schemes because they are sharing

the same mechanism.

The operation of hybrid DF/CF relaying in the first phase is the same as any non-hybrid one. However, during phase 2, the RN starts by trying to decode the received message and re-encodes and forwards it once the decoding is successful; otherwise, it compresses and forwards its observation instead. In other words, RN's transmission depends on its decoding results and the destination receives

$$y_d^2[i] = \begin{cases} \frac{c_0}{\sqrt{K_t d_0^{\zeta/2}}} x^2(w)[i] + \frac{c_2}{\sqrt{K_t d_2^{\zeta/2}}} x_r(w)[i] + z_d[i], & \text{if } \alpha BI(X^1; Y_r) \geq \frac{W}{T} \\ \frac{c_0}{\sqrt{K_t d_0^{\zeta/2}}} x^2(w)[i] + \frac{c_2}{\sqrt{K_t d_2^{\zeta/2}}} x_r(v)[i] + z_d[i], & \text{otherwise.} \end{cases} \quad (1.21)$$

where $I(X^1; Y_r)$ is the achievable rate of the S-RN link and is given as

$$I(X^1; Y_r) = \log_2 \left(1 + \frac{|c_1|^2 P_s}{N_0 B K_t d_1^{\zeta}} \right), \quad (1.22)$$

and T is the duration of the whole frame. It leads to the rate

$$R_{CDF} = \begin{cases} R_{DF}, & \text{if } \alpha BI(X^1; Y_r) \geq \frac{W}{T} \\ R_{CF}, & \text{otherwise.} \end{cases} \quad (1.23)$$

1.2.3 Energy Efficiency Analysis

The total energy consumption of a relay system is composed of both transmission power and circuitry energy consumption of all involved nodes. It should be noted that the optimization of a system's energy efficiency must be subject to certain quality of service (QoS) constraint. In this chapter, the QoS constraint to be satisfied by a communication system is defined in terms of the maximum tolerable probability of unsuccessful reception of a message, i.e. target outage probability.

Let us define the average transmission energy consumed by a two node system for transmission of one bit as E_b , the overall energy efficiency optimization should take into account circuitry power consumption. This optimization problem can be described as following: given the QoS constraint in terms of target outage probability and the packet duration con-

straint, find the optimal transmission energy E_b and packet duration T . It can be generally formulated as

$$\begin{aligned} & \text{minimize } E(E_b, T) & (1.24) \\ & \text{subject to } p_{out} \leq p_t, T \leq T_{max}, \end{aligned}$$

where p_{out} is the outage probability, p_t is the target outage probability and T_{max} is the maximum transmission time of each frame. However, in a three node relay-assisted system, not only the transmission energy E_b of the source should be optimized, but RN's E_b should also be optimized as well. The problem amounts to

$$\begin{aligned} & \text{minimize } E(E_{b,s}, E_{b,r}, T) & (1.25) \\ & \text{subject to } p_{out} \leq p_t, T \leq T_{max}, \end{aligned}$$

where $E_{b,s}$ and $E_{b,r}$ are the transmission energy per bit at the source and RN, respectively. In the following parts, we will study the energy efficiency of various relaying schemes.

AF : Define the transmission energy per bit at the source during phase 1 as $E_{b,s}^1$. In the first phase, the source broadcasts and the RN and the destination receives. In order to transmit message w with W bits, the source spends energy $WE_{b,s}^1$. In addition, the transmitting electronic circuitry of the source also contributes energy $P_{ct}T/2$ to total energy expenditure. Here P_{ct} is the power (in Watts) consumed by the transmitting electronic circuitry. The total energy expenditure needs to take both the transmission and reception sides into account. In particular, the electronic receiving circuitries of the RN and the destination also consume energy $P_{cr}T/2$ per node, where P_{cr} measures power (in Watts) consumed by receiving circuitries. Here we made two assumptions:

1. The transmitting circuitries of the source and the RN consumes the same amount of power;
2. The receiving circuitries of the RN and the destination consume the same amount of power.

These are simplified assumptions only for the purpose of theoretical analysis. More accurate power consumption models will be introduced later in the next section. The total energy consumption during phase 1 can be expressed as

$$E^1 = \left(W E_{b,s}^1 + \frac{P_{cr} T}{2} \right) + P_{cr} T, \quad (1.26)$$

where the first term in the parentheses is the total energy consumption on the transmitting side (source) and the second term stands for the energy consumption on the receiving side (RN and destination) during phase 1. During phase 2, the RN is actively transmitting as well as the source and the destination is the only receiving node. Suppose that the source spend $E_{b,s}^2$ for each bit, the total energy consumption is given by

$$E^2 = \left(W E_{b,s}^2 + \frac{P_{cr} T}{2} \right) + \frac{(P_r + P_{cr}) T}{2} + \frac{P_{cr} T}{2}, \quad (1.27)$$

where P_r is the RN transmission power. The first and second terms are the source and RN energy consumption, respectively, and the last term stands for the energy consumed by the destination's receiving circuitry. Although the source might have different transmission energy per bit during two phases, it is more applicable to assume that its transmission power is constant during the whole frame, i.e.

$$P_s = P_s^1 = P_s^2, \quad (1.28)$$

where P_s^1 and P_s^2 are transmission power during phase 1 and 2, respectively, and

$$P_s^1 = \frac{W E_{b,s}^1}{\alpha T}, P_s^2 = \frac{W E_{b,s}^2}{(1 - \alpha) T}. \quad (1.29)$$

Since $\alpha = 1/2$ in AF, we have $E_{b,s} = E_{b,s}^1 = E_{b,s}^2$, the overall energy efficiency can be expressed in terms of Joule/bit as

$$\begin{aligned} E(E_{b,s}, E_{b,r}, T) &= \frac{2W E_{b,s} + W E_{b,r} + \frac{3}{2}(P_{cr} + P_{ct}) T}{W} \\ &= 2E_{b,s} + E_{b,r} + \frac{3(P_{cr} + P_{ct}) T}{2W}, \end{aligned} \quad (1.30)$$

where $E_{b,r} = (P_r T/2)/W$. The outage probability is given by

$$p^{out} = \Pr \left\{ \bar{R}_{AF}(\gamma_0, \gamma_1, \gamma_2) < \frac{W}{T} \right\}, \quad (1.31)$$

where γ_i are random variables and $\gamma_i = |c_i|^2$, $0 \leq i \leq 2$. Considering the complexity of the expression for $\bar{R}_{AF}(\gamma_0, \gamma_1, \gamma_2)$, it is difficult to calculate the closed-form expression for outage probability. We can resort to the characteristic function of $\bar{R}_{AF}(\gamma_0, \gamma_1, \gamma_2)$

$$\phi(s) = \mathbf{E} \left\{ \exp \left(-s \bar{R}_{AF}(\gamma_0, \gamma_1, \gamma_2) \right) \right\}, \quad (1.32)$$

where $\mathbf{E}\{\}$ is the expectation function and the expectation is with respect to γ_i . The outage probability can be expressed by the Laplace inversion formula

$$\begin{aligned} p^{out} &= \Pr \left\{ \bar{R}_{AF}(\gamma_0, \gamma_1, \gamma_2) < \frac{W}{T} \right\} \\ &= \frac{1}{2\pi j} \int_{d_1-j\infty}^{d_1+j\infty} \frac{\phi(s) e^{sW/T}}{s} ds, \end{aligned} \quad (1.33)$$

where d_1 is a proper constant and $j = \sqrt{-1}$. This integration can be approximated as [49]

$$\begin{aligned} p^{out} &= \frac{1}{2\pi j} \int_{d_1-j\infty}^{d_1+j\infty} \frac{\phi(s) e^{sW/T}}{s} ds \\ &= \sum_{i=1}^M K_i \frac{\phi(z_i T/W)}{z_i}, \end{aligned} \quad (1.34)$$

where z_i are the poles of the Padé rational function, K_i are the corresponding residues and M is an arbitrary integer that determines the approximation accuracy. Now we rewrite the trivial upper bound \bar{R}_{AF} as a function of packet duration T , $E_{b,s}$ and $E_{b,r}$

$$\bar{R}_{AF} = B \log_2 \left(1 + \frac{2\gamma_0 W E_{b,s}}{T N_0 B K_t d_0^\zeta} + \frac{2W E_{b,s} \left(\frac{\beta^2 \gamma_1 \gamma_2}{K_t^2 (d_1 d_2)^\zeta} + \frac{\gamma_0}{K_t d_0^\zeta} \right)}{T N_0 B \left(1 + \frac{\beta^2 \gamma_2}{K_t d_2^\zeta} \right)} \right), \quad (1.35)$$

where $E_{b,s} = (P_s T/2)/W$. It is easy to see that the outage probability is also a function of T , $E_{b,s}$ and $E_{b,r}$. With this dependence, the energy efficiency of AF can be explicitly optimized

as

$$\begin{aligned} & \text{minimize } E(E_{b,s}, E_{b,r}, T) & (1.36) \\ & \text{subject to } p_{out}(E_{b,s}, E_{b,r}, T) \leq p_t, T \leq T_{max}. \end{aligned}$$

DF : In DF, the duration of phase 1 is αT . The energy expenditure including circuitry energy consumption can be given by

$$E^1 = \left(W E_{b,s}^1 + \alpha P_{ct} T \right) + 2\alpha P_{cr} T. \quad (1.37)$$

where the first two terms in the parentheses account for energy consumed for transmission of the message, mainly by the power amplifier, and the last term in the summation is the energy consumption of the receiving circuitries at the RN and the destination. During phase 2, the source and the RN transmit and the destination receives with total consumed energy

$$E^2 = \left(W E_{b,s}^2 + (1 - \alpha) P_{ct} T \right) + (1 - \alpha) (P_r + P_{ct}) T + (1 - \alpha) P_{cr} T. \quad (1.38)$$

Let $P_s = P_s^1 = P_s^2$, the overall energy efficiency is expressed as

$$\begin{aligned} E(E_{b,s}, E_{b,r}, T) &= \frac{\frac{W E_{b,s}}{\alpha} + W E_{b,r} + (2 - \alpha) P_{ct} T + (1 + \alpha) P_{cr} T}{W} & (1.39) \\ &= \frac{E_{b,s}}{\alpha} + E_{b,r} + \frac{(2 - \alpha) P_{ct} T + (1 + \alpha) P_{cr} T}{W}, \end{aligned}$$

where $E_{b,s} = E_{b,s}^1$.

The outage events of DF can be classified into two categories: RN outage and destination outage. RN outage refers the case where the RN detects an erroneous message. Forwarding this erroneous message to the destination will corrupt rather than help the final joint decoding, leading to unsuccessful reception. The probability of this kind of outage event is given by

$$\Pr(\text{relay outage}) = \Pr\left(R^1 < \frac{W}{T}\right) \quad (1.40)$$

$$= 1 - \exp\left(-\frac{N_0BK_t d_1^\zeta}{P_s} \left(2^{\frac{W}{\alpha TB}} - 1\right)\right).$$

Destination outage accounts for the events that the RN decodes and forwards correct information but the destination detects errors. The probability is

$$\begin{aligned} \Pr(\text{destination outage}) &= \Pr\left(R^1 \geq \frac{W}{T}, R^2 < \frac{W}{T}\right) \\ &= \Pr\left(R^1 \geq \frac{W}{T}\right) \Pr\left(R^2 < \frac{W}{T}\right), \end{aligned} \quad (1.41)$$

where R^1 is a function of γ_1 , and R^2 is a function of γ_0 and γ_2 , therefore independent with R^1 . These two categories of outage events are mutually exclusive and the overall outage probability is given as

$$p^{out} = \Pr(\text{relay outage}) + \Pr(\text{destination outage}). \quad (1.42)$$

In order to calculate $\Pr(R^2 < W/T)$, we can also use the Laplace inversion of characteristic function method. The optimization takes the same format as AF in equation.

CF : Following the same line of argument, the overall energy efficiency of CF is

$$E(E_{b,s}, E_{b,r}, T) = \frac{\frac{WE_{b,s}}{\alpha} + (1 - \alpha)P_t T + (2 - \alpha)P_{ct} T + (1 + \alpha)P_{cr} T}{W}. \quad (1.43)$$

In contrast to AF or DF, rather than forwarding a W bit message during phase 2, the RN forwards its compressed observation to be reconstructed by the destination. The compression rate determines the number of bits required for reconstruction, denoted by S_c . Equation (1.18) gives the constraint of the maximum bits that can be successfully transmitted in the RN to destination link

$$S_c = (1 - \alpha)BTR_0. \quad (1.44)$$

The above equation implies that the required number of bits S_c is a function of the instantaneous qualities of the RN to destination and source to destination links. The overall energy

efficiency can be given as

$$E(E_{b,s}, E_{b,r}, T) = \frac{E_{b,s}}{\alpha} + \frac{S_c E_{b,r}}{W} + \frac{(2-\alpha)P_{ct}T + (1+\alpha)P_{cr}T}{W}, \quad (1.45)$$

where $E_{b,r} = (1-\alpha)P_rT/S_c$. Note that with fixed transmission energy per bit, the transmission power is fixed at the source but adaptively adjusted because S_c is based on current channel condition at the RN.

The outage probability can be easily obtained as

$$p^{out} = \Pr\left(R_{CF} < \frac{W}{T}\right), \quad (1.46)$$

which can also be approximated by the same method discussed previously.

Hybrid Schemes : Depending on the decoding status at the RN, DF or CF is employed in hybrid relaying. When the RN detects error, it compresses and forwards its reception and the energy efficiency takes the form of equation (1.45). When RN's decoding is successful, DF is envisaged and the energy efficiency is given by (1.39). The average energy efficiency is the weighted summation of (1.39) and (1.45)

$$\begin{aligned} E(E_{b,s}, E_{b,r}, T) &= \Pr\left(R^1 < \frac{W}{T}\right) \left(\frac{E_{b,s}}{\alpha} + \frac{S_c E_{b,r}}{W} + \frac{(2-\alpha)P_{ct}T + (1+\alpha)P_{cr}T}{W}\right) \\ &\quad + \Pr\left(R^1 \geq \frac{W}{T}\right) \left(\frac{E_{b,s}}{\alpha} + E_{b,r} + \frac{(2-\alpha)P_{ct}T + (1+\alpha)P_{cr}T}{W}\right) \\ &= \frac{E_{b,s}}{\alpha} + \frac{(2-\alpha)P_{ct}T + (1+\alpha)P_{cr}T}{W} + \left(\Pr\left(R^1 < \frac{W}{T}\right) \left(\frac{S_c}{W} + 1\right)\right) E_{b,r}. \end{aligned} \quad (1.47)$$

The outage probability in the CF mode and DF mode are given, respectively, as

$$\begin{aligned} p_{CF}^{out} &= \Pr\left(R^1 \leq \frac{W}{T}, R_{CF} < \frac{W}{T}\right), \\ p_{DF}^{out} &= \Pr\left(R^1 \geq \frac{W}{T}, R^2 < \frac{W}{T}\right). \end{aligned} \quad (1.48)$$

Considering two modes are mutually exclusive, the overall outage probability is

$$p^{out} = p_{CF}^{out} + p_{DF}^{out}. \quad (1.49)$$

1.2.4 Insights and discussions

We optimize the energy per bit for both the source and relay and compare the energy efficiency performance of various strategies. We assume that the source, RN and the destination are placed in a straight line. The distance between the source and the destination is r and the RN is in the middle with distance $0.9r$ from the source and $0.1r$ from the destination. We use the typical power model settings in [41]: $W=10$, $P_{ct}=98\text{mW}$, $P_{cr}=112.4\text{mW}$, $K_t=6.05 \times 10^9$, $\zeta=3$, $N_0=-171\text{dBm/Hz}$, $B=1$ and $T_{max}=10$.

Figure (1.4) shows the situation where the S-D distance is short ($r \leq 100\text{m}$). The direct transmission is more efficient than any of the cooperative strategies until the S-D distance r is around 90m. The reason is that in small distance the circuitry energy consumption is the major part of the overall energy consumption. If the relay is activated, although the transmission energy per bit can be reduced, the overall circuitry consumption is almost doubled. Thus, to optimize the energy consumption, the relay should be de-activated to save the energy. When the S-D distance is increased ($r > 100\text{m}$) in figure (1.5), circuitry energy consumption becomes minor and the relay is able to help to reduce the overall energy per bit more efficiently. Among all the relaying strategies, the CF/DF based strategy has the best energy efficiency performance. When α is fixed, the AF/DF based strategy shows better energy efficiency than the DF based one. We can name, for each cooperative strategy, the point where it shows better energy efficiency performance than direct transmission as the switching point. As shown in the figure (1.5), the switching point of the hybrid CF/DF strategy is much smaller than other strategies.

Based on these results, we can conclude that the hybrid relay system that enables a pair of terminals (relay and destination) to exploit spatial diversity shows significant improvement in energy efficiency performance in terms of consumed energy per bit. However, compared with direct transmission, the cooperative strategy only shows improved energy efficiency when the destination is not very close to the source. Furthermore, it should be emphasized that this conclusion is highly depending on the energy consumption model adopted. These issues will be considered in the next sections.

1.3 H-ARQ Relaying and H²-ARQ Relaying

In this section, relaying schemes will be investigated in a packet-oriented data communication system, where retransmission protocols are needed. We analyze the Hybrid Automatic Repeat re-Quest (HARQ) protocols used in conjunction with non-hybrid and hybrid relaying schemes from the energy efficiency perspective. If the relaying schemes are non-hybrid, this combined strategy is named as H-ARQ relaying; otherwise, it is called H²-ARQ relaying since both the retransmission protocols and relaying schemes are hybrid.

Despite the exploitation of an efficient cooperative relaying strategy the transmitted packet might be lost due to the instantaneous channel condition and noise realization. The packet loss could be even more severe when the system is operating under static (block) fading condition and the transmitter is not able to properly tune its transmission rate due to the lack of sufficient level of channel knowledge. Retransmission techniques based on automatic repeat request, i.e. ARQ [50]- [52] and its advanced hybrid types that combine forward error correction (FEC) with ARQ by keeping previously received packets for detection, commonly known as hybrid ARQ (HARQ), will be the natural choices to circumvent this problem and guarantee correct data packet delivery to the final destination. Common encoding techniques for HARQ are repetition coding (RC) with chase combining and unconstrained coding (UC) with incremental redundancy (INR) respectively [53]- [55]. The emphasis of this section is on HARQ, specifically INR as it is capable of offering higher throughput [56]. As the repetition coding based HARQ performs weaker than INR and the extension of the presented analysis to repetition coding is a straightforward practice, it will not be considered in this section.

Being a technology that spans both the MAC and physical (PHY) layers, HARQ protocols are of great interest to be examined. Some studies of HARQ protocols regarding throughput analysis, error rate and average delay in two-node communications can be found in [56]- [57]. The combination of cooperative communications and HARQ has been investigated in [58]- [61]. In [58], the diversity-multiplexing-delay tradeoff was analyzed and two kinds of diversity including space and ARQ diversity were exploited. Lin Dai studied the application of adaptive cooperation with ARQ in [59], where the relay will not be involved in the cooperation if errors are detected. The work has been further extended to HARQ

in [62]- [63] and [9]. In [9], the energy consumption of a DF based HARQ system is analyzed. However, in these previous works, HARQ is deployed with a non-hybrid forwarding scheme, usually DF, and hence referred as H-ARQ-Relaying. As shown by pervious results, we know that the outage behavior can be greatly improved if the relay adaptively switches between different forwarding schemes. Further improvement can be expected by combining a hybrid relay system with HARQ. This combined strategy is called H²-ARQ-Relaying since both the retransmission protocols and the relaying schemes are hybrid. In [62], the HARQ strategy is deployed in a relay system where the relay is allowed to switch between AF and DF. Compared with conventional HARQ strategies based on DF only, the new relay system is able to enjoy certain level of flexibility and exhibits significant improvement in FER.

In this section, we focus on the hybrid CF/DF based H²-ARQ-Relaying strategy, although the AF/DF one is also addressed briefly. Only incremental redundancy (INR) based HARQ is considered and the proposed strategies and their spectrum and energy efficiency analysis are the main topics.

1.3.1 H²-ARQ Relaying Strategy

When retransmission protocols are considered, the same message is transmitted until the destination successfully decodes it or the maximum retransmission limit is reached. In the l -th retransmission the signals received by the RN and the destination during the source broadcasting phase are

$$\begin{aligned} y_{r,l}[i] &= \frac{c_{1,l}}{\sqrt{K_t}d_1^{\zeta/2}}x_l^1(w)[i] + z_{r,l}[i], \\ y_{d,l}^1[i] &= \frac{c_{0,l}}{\sqrt{K_t}d_0^{\zeta/2}}x_l^1(w)[i] + z_{d,l}[i], \end{aligned} \quad (1.50)$$

respectively, where $1 \leq l \leq L$ and L is the maximum retransmission limit. As depicted in the right part of figure (1.6), the feedback channels are used to convey the decoding status at the relay and the destination.

If the message is successfully decoded by the destination, where the decoding is based

on all previously buffered signals, an acknowledgement (ACK) message is sent back to the source and the RN and the transmission of message w is finished. If the destination detects errors, it broadcasts a not acknowledgement (NAK) message. Once the relay receives the NAK message, it tries to decode. Different actions are envisaged based on its decoding status:

Relay Decoding Success : An ACK is broadcast by the RN to indicate that it will employ the DF mode. The source and the RN then transmit $x_l^2(w)$ and $x_{r,l}(w)$, respectively, and the destination receives

$$y_{d,l}^2[i] = \frac{c_{0,l}}{\sqrt{K_t d_0^{\zeta/2}}} x_l^2(w)[i] + \frac{c_{2,l}}{\sqrt{K_t d_2^{\zeta/2}}} x_{r,l}[i] + z_{d,l}[i]. \quad (1.51)$$

Afterwards, the source keeps silent during phase 1 of the following frames to save the energy. It only transmits with the RN in a more efficient cooperative manner during phase 2 until the source receives ACK or the retransmission limit N is reached.

Relay Decoding Failure : The relay switches to the CF mode and broadcasts a NAK message. At the end of phase 2, the destination attempts to decode by joint processing current and previous receptions. Upon successful decoding, an ACK is sent back; otherwise, the destination issues a NAK message to start a new frame if $l < L$. If $l = L$, HARQ failure is announced. In this H²-ARQ-Relaying strategy, we need to consider five possible scenarios as follows:

1. Case 1: the information message w is successfully decoded by the destination at the end of phase 1 in the l -th frame. An implication of this scenario is that in previous $l-1$ transmission, the RN cannot decode and CF is conducted.
2. Case 2: the RN cannot decode but successful decoding occurs at the destination after l CF operations.
3. Case 3: the DF mode is activated in the i -th frame and the destination correctly decodes w in the l -th frame.
4. Case 4: after maximum retransmission, neither the RN nor the destination can decode.

5. Case 5: the DF mode is activated in the i -th frame but the destination cannot correctly decode w after L retransmission.

State diagram composed of a finite number of states can be used to describe the behavior of a system and analyze and represents the events of the system. The H²-ARQ-Relaying can also be represented by a state diagram presented in figure (1.7) to demonstrate the process. B_l stands for the state where the source is ready to broadcast w in the l -th frame. The state D_l indicates that the DF mode is activated at the end of phase 1 of the l -th frame. $DF_{m,l}$ is the state where the system has entered the DF mode in the l -th frame and cooperative transmission in phase 2 has been repeated m times but the destination still detects errors. C_l defines the state in which the relay is ready to conduct CF during phase 2 of the l -th frame. S and F_a are the successful decoding state and HARQ failure state, respectively.

1.3.2 Performance Analysis

Each state in figure (1.7) represents different transmission rate achieved and amount of energy expenditure consumed. In order to investigate the average behavior in terms of spectrum and energy efficiency for the H²-ARQ-Relaying strategies, we first need to derive the state and transition probabilities of the state diagram. The outage probability introduced and derived in the previous section will help us to find the state and transition probabilities.

Caire has pointed out that the INR based HARQ sends additional coded symbols (redundancy) until successful decoding is achieved [56]. After l transmission, the achievable rate at the destination is expressed as

$$R_d(l) = \sum_{i=1}^l R_{d,i}, \quad (1.52)$$

where $R_{d,i}$ stands for the achievable rate in the i -th frame and can either take the form of equation (1.12) or (1.16) according to DF or CF operation is conducted. Similarly, the achievable rate at the RN is

$$R_r(k) = \alpha B \sum_{i=1}^k \log_2 \left(1 + \frac{|c_{1,i}|^2 P_s}{N_0 B K_t d_1^{\zeta}} \right). \quad (1.53)$$

We define the outage the event $A_{l,k} = R_d(l) < W/T, R_r(k) < W/T$. The outage probability $\Pr(A_{l,k})$ can be calculated by resorting to the 2-dimensional characteristic function of $R_d(l)$ and $R_r(k)$,

$$\begin{aligned} \Psi(\mathbf{s}, l, k) &= \mathbf{E} \{ \exp(-s_1 R_d(l) - s_2 R_r(k)) \} \\ &= \mathbf{E} \left\{ \prod_{i=1}^k \exp(-s_1 R_{d,i}(l) - s_2 R_{r,i}(k)) \prod_{i=k+1}^l \exp(-s_1 R_{d,i}(l)) \right\}, \end{aligned} \quad (1.54)$$

where \mathbf{s} is (s_1, s_2) . The outage probabilities can be expressed by the Laplace inversion formula of $\Psi(\mathbf{s}, l, k)$ and approximated as [49],

$$\begin{aligned} \Pr(A_{l,k}) &= \frac{1}{(2\pi j)^2} \int_{d_2-j\infty}^{d_2+j\infty} \int_{d_1-j\infty}^{d_1+j\infty} \frac{\Psi(\mathbf{s}, l, k) e^{\frac{s_1 W}{T} + \frac{s_2 W}{T}}}{s_1 s_2} ds_1 ds_2 \\ &\approx \sum_{i=1}^M \sum_{j=1}^M K_i K_j \frac{\Psi(\mathbf{z}, l, k)}{z_i z_j}, \end{aligned} \quad (1.55)$$

where \mathbf{z} is $(z_i T/W, z_j T/W)$. This approximation can be easily extended to the AF/DF-based strategy, where CF is replaced by AF.

For two events sets e_1 and e_2 , if $(e_1 \subseteq e_2)$, $\Pr(e_1, e_2)$ is equal to $\Pr(e_1)$. In the state diagram, the transition probability to state j from any of its adjacent incoming state i is

$$\Pr(\text{state } i \rightarrow \text{state } j) = \Pr(\text{state } j | \text{state } i) = \frac{\Pr(\text{state } j)}{\Pr(\text{state } i)}. \quad (1.57)$$

In the state diagram, all the states have this property except the state S . Therefore we can first calculate the state probabilities and then obtain the transition probabilities based on (1.57). For instance, $\Pr(B_l)$ can be easily obtained as $\Pr(A_{l-1, l-1})$. Other state probabilities can be obtained by manipulating $\Pr(A_{l,k})$ we well. With state probabilities, transition probabilities can be further derived. One useful trick to reduce the complexity is to use the fact that the probabilities of all the state transitions emanating from a single state must add up

to 1. For instance, we have

$$\Pr(B_l \rightarrow S) = 1 - \Pr(B_l \rightarrow D_l) - \Pr(B_l \rightarrow C_l). \quad (1.58)$$

The spectrum efficiency is evaluated by the expected throughput in terms of bit/second. Unlike previous section, here we use total amount of bits delivered per unit energy expenditure to evaluate the energy efficiency to give a fresh view.

Using the state and transition probabilities, we can apply the renewal-reward theorem [56] to evaluate the throughput by investigating the random reward Φ and average airtime T_{air} . In case 1, CF is used in previous $l-1$ transmission, the total airtime is clearly $(l-1)T$ and the total energy consumption is $(l-1)WE(E_{b,s}, E_{b,r}, T)$, where $E(E_{b,s}, E_{b,r}, T)$ takes the form of (1.45). The l -th frame consists of a source broadcasting phase only. The airtime and energy consumption are αT and E^1 , respectively. The overall average time and energy expenditure associated with case 1 is given by

$$\begin{aligned} T_1 &= T \sum_{l=1}^L P_{BS}(l) ((l-1) + \alpha), \\ E_1 &= \sum_{l=1}^L \left((l-1)E_{CF}W + E^1 \right), \end{aligned} \quad (1.59)$$

respectively, where E_{CF} and E^1 are given in (1.45) and (1.37), respectively, and $P_{BS}(l) = \Pr(B_l)\Pr(B_l \rightarrow S)$. Following the same line of argument, the average air time and energy expenditure can also be derived for other four cases. For the purpose of conciseness, their expressions are not shown in this book but readers can refer to [12] for details.

The average airtime is the weighted summation

$$\mathbf{E}\{T_{air}\} = \sum_{i=1}^5 T_i. \quad (1.60)$$

The average reward is

$$\mathbf{E}\{\Phi\} = (1 - p^{out})W, \quad (1.61)$$

where p^{out} is the probability that the decoding is still unsuccessful after maximum retransmission and given by

$$p^{out} = \Pr(F_a) + \sum_{N=1}^L \Pr(DF_{L-N+1,N}). \quad (1.62)$$

The average throughput is

$$\eta = \frac{\mathbf{E}\{\Phi\}}{\mathbf{E}\{T_{air}\}}. \quad (1.63)$$

The total amount of bits delivered is W and bits to energy expenditure ratio reads

$$C_J = \frac{W}{\sum_{i=1}^5 E_i}. \quad (1.64)$$

Apparently, C_J is still a function of $T, E_{b,s}$, and $E_{b,r}$ and it can be optimized subject to the outage probability and transmission time constraints as we did in previous section. However, due to the complexity of the problem, this optimization problem has to be solved numerically.

1.3.3 Insights and Discussions

We provide some results for the proposed strategies and compare their performance with some benchmark ones. The maximum retransmission limit L is set to 4. The benchmark strategies and their abbreviations are listed as follows:

1. H-ARQ with direct transmission (DT): The relay keeps silent throughout the transmission.
2. H-ARQ-Relaying with the co-located relay and destination (CRD): We assume that the relay and the destination are connected by a wire such that full receive diversity is achieved.
3. H-ARQ-Relaying with conventional DF (DF): When the relay detects errors, it keeps silent during phase 2; otherwise, the relay and the source transmit simultaneously.
4. H²-ARQ-Relaying with hybrid AF/DF (HAD): The relay performs AF when detecting errors and DF when successfully decoding. Note that in this case, α is also fixed at 0.5

and repetition coding is used when AF is performed.

The CF/DF-based strategy is denoted as *HCD*. The source and the destination are assumed to be placed in the foci of the ellipse $(d/r)^2/(e/2)^2 + (y/r)^2/(b/r)^2 = 1$, for $1 < e < +\infty$. The relay is moving along the ellipse. With this assumption, we are able to investigate the relay system's performance when the relay is not on the line segment between the source and the destination. The same power model is used here.

Comparison of Spectrum Efficiency

Figure (1.8) gives the throughput of strategies with respect to d/r . Basically, the throughputs are upper bounded by *CRD* because it is able to enjoy full receive diversity. The CF/DF-based strategy is the closest one to *CRD*. It can be interpreted as follows: when the relay is moving towards the destination, the S-RN link is getting less reliable and the successful decoding probability at the relay decreases. In such a scenario, if the system uses DF, it is more likely that the relay's decoding fails and the system operates in direct transmission mode during phase 2, thus no diversity can be achieved. In contrast, when the hybrid CF/DF scheme is used, the system will be able to achieve receive diversity through CF. As far as HAD is concerned, it enjoys a certain level of flexibility and its throughput is improved in comparison with *DF* when α is fixed at 0.5. However, when the S-RN link is of low quality, the relay forwards nothing but mostly its own noise. In addition, *HAD* suffers from the bandwidth loss due to the use of repetition coding, and its throughput is therefore lower than *DF* with optimal α . Another common trend of strategies is that when the relay moves away from the source, their throughputs decrease. For *DF*, this can be explained by the smaller decoding probability of the relay, which causes fewer opportunities for the relay to cooperate. For *HCD*, although CF can be used, the achievable rate depends on the quality of the S-D and S-RN links. The average SNR of the S-RN link is decreasing when the relay moves towards the destination. Hence, the throughput reduces. The AF/DF-based strategies can be explained following the similar argument.

Comparison of Energy Efficiency

We optimize the energy per bit for both the source and the relay and compare the energy efficiency performance of various strategies when the relay is close to the destination (the S-D link and RN-D link are vertical to each other). Figure (1.9) shows the situation where the S-D distance is from short ($r < 100\text{m}$) to long ($100\text{m} < r < 1000\text{m}$). The direct transmission is more efficient than any of the cooperative strategies in terms of the energy per bit in short range. The reason has been explained before. Thus, to optimize the energy consumption, the relay should be de-activated to save the energy. The DF-based strategy consumes less energy than others because in this strategy, the relay is silent when detecting errors and the circuitry energy consumption is saved, while in the hybrid strategies, the relay still transmits, leading to extra circuitry energy consumption. When the S-D distance is increased ($r > 100\text{m}$) in figure (1.10), circuitry energy consumption becomes minor and the relay is able to help to reduce the overall energy per bit. The CF/DF-based strategy has the best energy efficiency performance.

In this section, we propose novel Hybrid Automatic Repeat re-Quest (HARQ) strategies used in conjunction with hybrid relaying schemes, named as H²-ARQ-Relaying. The strategies allow the relay to dynamically switch between amplify-and-forward/compress-and-forward and decode-and-forward schemes according to its decoding status. The spectrum efficiency of the proposed strategies, in terms of the maximum throughput, is significantly improved compared with their non-hybrid counterparts under the same constraints. The consumed energy per bit is optimized by manipulating the node activation time, the transmission energy and the power allocation between the source and the relay. Numerical results lead to the same conclusion that cooperative HARQ is energy efficient in long distance transmission only.

1.4 Energy Efficient RNs in Cellular Networks

With the previous discussion as basis, this section will study the energy saving potential of relaying schemes in cellular systems. RNs are added for incremental capacity growth, richer user experience and in-building coverage. In particular, RNs are deployed as complementary

sites to Macro BSs to improve the cell edge performance, which is one of the main challenges faced by the developing standards. They are normally offering flexible site acquisition with low power consumptions and, using over-the-air link as backhaul connection to the base stations, providing coverage extension and capacity enhancement with little to no incremental backhaul expense as shown in figure (1.11). They are especially suitable for the scenarios where terrestrial condition is too harsh for wired backhaul connections.

The first commercial standard incorporating relaying technology is IEEE.801.16j [36]. The relay group developed new BS and RN capabilities to enable relay networks to be realized and provide support for access by legacy devices. Two different operating modes are provided: transparent mode and non-transparent mode. LTE-A is also considering using relaying technology for cost-efficient throughput enhancement and coverage extension and more sophisticated relaying strategies are being incorporated [38].

RNs cover much smaller area than macro BSs. They may have additional transmission power compared to terminals and yet be much lower compared to a base station because of their limited functionality and lower transmission power. Thus a more energy efficient power consumption model is expected for RNs and as a consequence they can be promising solution for 'green' cellular networks. However, as we discovered in previous results, relay is not always able to help and to what level it can help is highly depending on the power model, RN's location and number of RNs deployed. The objective of optimizing the usage of RNs needs to answer at least two following questions:

1. How many RNs are needed to minimize the energy usage?
2. What are the optimum locations for these relay nodes in order to reduce the energy consumptions

The rest of the section will address these two questions first and extend our study to other interesting topics such as the comparison of indoor and outdoor relay applications.

1.4.1 Cellular System and Power Model

Before we can investigate the relay-assisted cellular system, we need to introduce the basic concept of a cellular network as well as introducing a well defined power model. A cellular network is defined as a radio network distributed over cells which are joined together to provide radio coverage over a wide geographic area. In this paper, each cell consists of three sectors and each sector is defined as a hexagon with radius R as shown in figure (1.11). The BSs are located in the center of each cell and consist of three directional antennas, each serving a different sector of the cell. The antenna pattern is given as [64]

$$G(\Theta) = G_{max} - \min \left\{ 12 \left(\frac{\Theta}{\Theta_{3dB}} \right)^2, G_{f2b} \right\} \quad (1.65)$$

$$G_{max} = 14dB, \Theta_{3dB} = 65^\circ, G_{f2b} = 20dB,$$

where G_{max} is the boresight antenna gain, Θ is the angle between the sector and the mobile (BS-UE) line of sight and the sector boresight, Θ_{3dB} is the 3 dB angle, also defined as beam-width in this work, and G_{f2b} is the antenna front to back ratio.

The RNs are placed in some specific positions as shown in figure (1.12). There could be multiple RNs in each sector. In such a case, some interference coordination mechanism between RNs might need to be considered. We assume that each RN has an omni-directional antenna.

Normally, the received signal from a BS suffers from path-loss, slow fading and fast fading. A simple model taking path-loss into consideration is given as [64]

$$PL(dB) = 15.3 + 37.6 \log_{10}(d), \quad (1.66)$$

where d is the BS-UE distance in meters. The shadowing $SF(dB)$ follows a log-normal law with mean 0 and shadowing standard deviation SD . Based on this propagation model, the long-term power received by a UE from a BS (BS_i) can be expressed in dB as

$$P(BS_i \rightarrow UE) = P_{Tx} + G_{UE} + G - PL(d) - SF(BS_i \rightarrow UE), \quad (1.67)$$

where P_{Tx} is the transmission power of the BS, G is the antenna gain, d is the BS-UE distance and $SF(BS_i \rightarrow UE)$ is the (correlated) shadowing in dB between the BS and the UE. We can introduce coverage defined as the fraction of cell area where the received power is above certain threshold. However, in this work, we use another commonly used metric of interest G_{factor} to evaluate coverage

$$G_{factor} = \frac{P(BS_i \rightarrow UE)}{\sum_{j \neq i} P(BS_j \rightarrow UE) + P_{therm}}, \quad (1.68)$$

where $P(BS_i \rightarrow UE)$ is given in mWatts and P_{therm} is the thermal noise power given in mWatts. The long-term coverage is defined as

$$Cov = \frac{1}{S_a} \int_{S_a} \Pr \{G_{factor}(x, y) \geq G_{factor,min}\} dx dy, \quad (1.69)$$

where S_a is the area of a sector.

An accurate power model is essential to evaluate the energy efficiency of a system. Since the energy consumption estimation mainly involves BSs and RNs, we set up two different power models for each type of nodes. A general power model has been given in [65], where a high-level block diagram with the main radio sub-systems is defined and the power consumption of each sub-system is calculated individually.

As shown in figure (1.13), the power consumption is stemming from multiple subsystems including a lossy Antenna Interface (AI), a Power Amplifier (PA), a Radio Frequency (RF) small-signal transceiver section and a baseband interface (BB), a DC-DC power supply regulation, an active cooling system and finally a main AC-DC power supply for connection to the electrical power grid. The overall power consumption can be broke down in subsystem level to illustrate each subsystem's influence more precisely.

A state-of-the-art energy consumption estimation for a typical commercial BS is given in table (1.1) as well as the power consumption breakdown figure (1.14).

It is interesting to note that in Macro BSs it is mainly the PA that dominates the total power consumption, owing to the high antenna interface losses.

The RN power consumption model is established in [66] and given in table (1.2). The power breakdown figure (1.15) shows that the main source for power consumption is still the PA. Generically speaking, RNs have significantly lower transmission power, thus consumes much less energy compared to macro BSs. The well-timed power model will form the basis for the energy efficiency study afterwards.

1.4.2 Optimization of RN Deployment

The link level results have revealed that the locations of RNs play an important role in the overall energy efficiency. In cellular systems, the number of RNs deployed in one sector is also an interesting topic worthy of being studied. Most of the analysis in this chapter focuses on downlink communication. Still communication takes place in two orthogonal phases. In the first phase, the BS transmits while the RN and the UEs receive, and in the second phase the BS and the RN transmit while the UEs receive. We assume that the phases are synchronized so that the first phase and second phase occur simultaneously in all cells.

Assuming that all BSs transmit at the same time and frequency with maximum power, and that the cellular architecture is such that each cell sees the same interference, i.e. neglecting network edge effects, we can focus on a single sector of a single cell. We start from the scenario that there is only one RN associated with each sector and extend out discussion to multiple RNs afterwards.

We start from single RN case. During the first phase, the RN in sector j receives (time indices of the symbols are removed for ease of notation)

$$y_{r,j} = h_j x_{s,j}^1 + \sum_{k \in \Omega, k \neq j} h_k x_{s,k}^1 + z_r, \quad (1.70)$$

where h_j is the sector j to RN channel (the path-loss, shadowing, antenna gain and etc. are absorbed for ease of notation), $x_{s,j}$ is the transmitted signal from sector j , z_r is the additive Gaussian thermal noise at RN, Ω is the set of all interfering sectors, and superscript stands for phase. Here the second term actually represents the summation of two parts: the intra-cell interference from other sectors within the same BS and inter-cell interferences from the

sectors of other BSs. They can be treated in the same way. It should be noted that we do not take RNs in other sectors as interfering nodes because their transmission power is very low compared to the BSs and the interference generated can be ignored. We further assume that only one UE is served by RN in each sector, the received signal is

$$y_{UE,j}^1 = h_{UE,j}x_{s,j}^1 + \sum_{k \in \Omega, k \neq j} h_{UE,k}x_{s,k}^1 + z_{UE}, \quad (1.71)$$

where $h_{UE,j}$ is the sector j to UE channel and z_{UE} is the additive Gaussian thermal noise at UE. During phase 2, the BS and the RN transmit and the UE receives

$$y_{UE,j}^2 = h_{UE,j}x_{s,j}^2 + h_{UE,r}x_r + \sum_{k \in \Omega, k \neq j} h_{UE,k}x_{s,k}^2 + z_{UE}, \quad (1.72)$$

where $h_{UE,r}$ is the RN to UE channel. The UE then jointly processes $y_{UE,j}^1$ and $y_{UE,j}^2$ to decode the message, depending on the forwarding scheme employed by the RN. With a similar approach to that followed for the achievable rate derivation, and considering the power consumption model, in each point of the sector the Shannon Capacity and the energy consumption per bit of different relaying schemes can be evaluated. We define the average energy efficiency as

$$E_{ave} = \frac{\text{total energy consumption}}{\text{average capacity within a sector}}. \quad (1.73)$$

Without considering fast fading, the equivalent G_{factor} is defined as a function of Shannon Capacity

$$G_{fac,eq} = 2^{C/B} - 1, \quad (1.74)$$

where C is the Shannon capacity at one point of the sector. We assume the inter-cell distance is 2000 meters. The the equivalent $G_{fac,eq}$ and energy consumption distributions are reported in figure (1.16)and (1.17), where DF is applied. If we set coverage threshold as 0dB, with the RN, the coverage can be improved 8%. However, energy consumption is not reduced but rather increased by using relay. With a RN, the system's capacity can be improved and extra amount of bits can be delivered. However, adding a RN to the network comes with a cost, i.e. extra energy consumption required for the RN. If the influence of the extra required energy outweighs the benefit, i.e. the improvement in capacity, the energy efficiency of the

network is actually degraded. This is exactly what happened in our case.

However, in figure (1.17), the RN is just randomly deployed in the sector and only DF is considered. The link level results have indicated that the distance, designated as d , between the source, i.e. BS, and the RN plays a key role in the overall system energy efficiency. Now we optimize the location of the RN and investigate how the energy efficiency is changed with location and forwarding schemes. Not that in a two dimensional cellular system, we need to consider the angle between the BS and the RN line of sight and the sector boresight as well, denoted as θ_r .

Figure (1.18) shows E_{ave} when the RN is moving away from the BS towards the sector edge along the direction with θ_r equal to 60 degrees. As we can see, the location of the RN changes the system's capacity as well as the energy efficiency. For a RN using DF, cell edge might not be a good option because it would be difficult for the RN to decode in such a long distance and the improvement of capacity is small. With extra energy required, the energy efficiency is degraded compared to no RN case. The optimal location is in the middle of the BS and the cell edge and, compared to no RN case, the energy efficiency is improved. With hybrid relaying, the energy efficiency can be further improved because the RN has the flexibility of choosing CF when decoding is difficult. The UE is benefiting from receive diversity when CF is used. The optimal location of hybrid relaying is close to the cell edge.

Now we move to multiple RN scenario. If phase synchronization is not achieved by the network, multiple RNs within the same sector can have different duplexing schedules which cause interference to each other when some RNs are in transmitting phase but others are in receiving phase. Even with phase synchronization, inter-RN interference can still exist when the same sub-carriers are used by different RNs. In this chapter, we assume that BSs uses some resource allocation schemes which guarantee the orthogonality of multiple RNs within in one sector. Since we only consider one UE scenario for simplicity, the UE owns all available resources and the assumption does not make any significant difference. However, in multiple UE case, a central or distributed resource allocation strategy needs to be employed and each RN can only have limited resources.

Supposing N_r RNs within one sector, during phase 1, the BS multicasts to RNs and UE,

the received signal at RN i is

$$y_{r,j \rightarrow i} = h_{j \rightarrow i} x_{s,j}^1 + \sum_{k \in \Omega, k \neq j} h_{k \rightarrow j} x_{s,k}^1 + z_{r,i}, \quad (1.75)$$

where $h_{j \rightarrow i}$ is the sector j to RN i channel, $z_{r,i}$ is the additive Gaussian thermal noise of RN i for $1 \leq i \leq N_r$. At the same time, the UE listens to the BS and it reads (1.71). The second phase has multiple sources and single destination. We consider the relay selection scheme (RSS). In RSS, the UE is associated with only one RN, denoted as active RN, which has the strongest RN to UE link and other RNs are in idle state. The active RN and BS transmit and the UE receives

$$y_{UE,j}^2 = h_{UE,j} x_{s,j}^2 + h_{UE,r,i} x_{r,i} + \sum_{k \in \Omega, k \neq j} h_{UE,k} x_{s,k}^2 + z_{UE}, \quad (1.76)$$

where $h_{UE,r,i}$ is the RN i to UE channel. Since the other RNs are not transmitting, they do not generate interference. The UE just acts in the same manner as it does in the single RN scenario. The selected RN can employ any forwarding scheme including a hybrid scheme. The capacity of a sector with two RNs is shown in figure (1.19).

As can be seen in figure (1.20), adding RNs can improve the capacity in the vicinity of the RN (here only path-loss is considered to give a clear picture). With multiple RNs, it is natural to spread the RNs evenly in a sector to balance the possibility of a UE served by a RN in the whole area. In this regard, we choose θ_r as

$$\theta_{r,i} = \frac{180^\circ}{N_r + 1} i, \text{ for } 1 \leq i \leq N_r. \quad (1.77)$$

We move the RNs from the BS towards the cell edge and show the average energy efficiency E_{ave} for $N_r=2, 4$ and 6 .

Using N_r RNs does not necessarily mean that the required energy for RNs is increased for N_r times. As we mentioned, RN selection is applied in this multiple RN scenario. Only the UE associated RN is actively receiving and transmitting while the other RNs are in the idle state. However, those RNs cannot be entirely switched off because a UE with mobility might need access at any time and thus some sub-systems are still working and consuming

certain amount of energy. The idle RN energy consumption can be obtained based on the RN power model and it will determine the optimal number RNs to be deployed. As shown in figure (refrelay2RN), increasing number of RNs is able to improve E_{ave} but the improvement is getting less. For instance, from 1 RN to 2 RNs E_{ave} is improved by about 5% but from 4 RNs to 6 RNs E_{ave} improvement is almost negligible. There are two consequences of deploying more RNs. One is that the system's capacity is improved and the other is that more energy is needed for those idle RNs. If the capacity improvement is more significant, E_{ave} can benefit; otherwise, it will suffer. Our results show that deploying more than 6 RNs in one sector might not be efficient from the energy and deployment cost points of view. The capacity improvement is very limited but the energy consumption is getting more and more significant.

1.4.3 Outdoor-to-Indoor Relaying

On the hand, the use of relay would tend to increase the overall network energy consumption, on the other hand, avoiding to waste large amount of power for transmitting through wall could save a lot more of energy. We investigate here the EE of in-building relaying scenario where a non-regenerative relay is used for relaying the signal of an outdoor BS to an indoor UE and, hence, the access link (RN-UE link) is more reliable than the donor link (BS to RN link) since the RN is meant to be close to the UE. Assuming this scenario, we can derive a simple close-form approximation of the channel capacity by following a similar approach based on random matrix theory as in [67], utilize it for defining the EE of this AF system and, then, comparing its EE against traditional point-to-point (P2P) communication.

In this study, we consider a cooperative MIMO AF system that is composed of three nodes, i.e. a BS with n antennas, a nonregenerative RN with q antennas and a DN with r antennas. For the simplicity of the introduction, we assume a half-duplex relaying scenario with two phases of equal duration. In the first phase, the BS broadcasts its signal to the RN and UE; in the second phase, the RN, which acts as a repeater, transmits an amplified version of the BS signal to the UE. We also assume that the access link is far more reliable than the other two links. In our model, the SNRs of the direct (BS-UE), donor and access

links are defined as γ_0 , γ_1 and γ_2 , respectively, and $\sigma = \gamma_0/\gamma_1$ stands for the SNR offset between the direct and donor links. According to this system model, it has been indicated in [68] that the maximum achievable SE of the MIMO AF can be approximated as

$$C \approx \frac{1}{2 \ln(2)} \left[n \ln \left(\frac{\gamma_0}{d_0} \right) + q \left(\ln(1 + \sigma d_0) + \frac{1}{1 + \sigma d_0} - 1 \right) + r \left(\ln(1 + d_0) + \frac{1}{1 + d_0} - 1 \right) \right] \quad (1.78)$$

when the access link quality is 20 dB higher than the donor link, i.e. $\gamma_2 \gg \gamma_1$, and for large values of n , q and r . In addition, d_0 is the unique nonnegative root of the following polynomial

$$P(d) = d^3 \lambda_1^2 + d^2 [\lambda_1 (\lambda_0 \lambda_1 (r+q-n) + \lambda_0 + \lambda_1)] + d [\lambda_0 \lambda_1 (1 + \lambda_0 (r-n) + \lambda_1 (q-n))] - n \lambda_0^2 \lambda_1, \quad (1.79)$$

where $\lambda_i = \gamma_i/n$, $i = \{0, 1\}$. The main purpose of (1.78) is the evaluation and comparison of the capacity of in-building MIMO AF systems in a faster way than time consuming Monte-Carlo simulations, and with a sufficient accuracy such that it can be used in network simulation and optimization. In addition, it can provide upper bounds on the achievable rate of generic cooperative MIMO AF systems. As far as the total power consumption of this MIMO AF system is concerned, it can be characterized as

$$P_{\Sigma,AF} = P_{BS,Tr} + P_{RN,Tr} + P_{RN,Re} + 2P_{UT,Re}. \quad (1.80)$$

according to the two-phase transmission model, where $P_{BS,Tr}$, $P_{RN,Tr}$, $P_{RN,Re}$ and $P_{UT,Re}$ are the consumed power relate to BS transmission, RN transmission, RN reception and UE reception, respectively. In [65], the total consumed power of several types of BS for both transmitting and receiving signals has been abstracted from real measurement (see Table 1.1 for macro BS) as

$$P_{BS} = t(\Delta_P P_1 + P_{Ov,BS}), \quad (1.81)$$

where t is the number of transmit antenna at the BS, Δ_P accounts for the power amplifier (PA) inefficiency and P_0 is the overhead power, i.e. signal processing overhead, cooling and power supply (PS) losses as well as current conversion losses (see Figure 1.13). In addition P_1 is the transmit power per PA, i.e. per antenna, at the BS and it varies from 0

to P_{\max} . In the updated version of [65], it has been shown that this linear abstraction can also be used for either rural or urban RNs based on the measurement of Table 1.2 such that $P_{RN} = t(\Delta_{P,RN}P_2 + P_{Ov,RN})$, where P_2 is the transmit power per PA at the RN. Moreover, the same linear type of power model has been used in [69] for characterizing the power consumption of a UE. Assuming the linear power model of (1.81) for each node, the total consumed power of the system in (1.80) can be re-expressed as

$$P_{\Sigma,AF} = n(\Delta_{P,BS}P_1 + P_{Ov,BS}) + q(\Delta_{P,RN}P_2 + P_{Ov,RN}) + q\varsigma P_{Ov,RN} + 2r\varsigma P_{Ov,UE}, \quad (1.82)$$

where $\varsigma \in [0, 1]$ characterizes the ratio between transmission and reception overhead power. Intuitively, less overhead power will be necessary for receiving than transmitting signals. The EE in bits/J/Hz of this system can be simply defined as the ratio of its SE in (1.78) to its total consumed power in (1.82) such that

$$C_J = \frac{C}{P_{\Sigma}}. \quad (1.83)$$

Using the values for P_{BS} and P_{RN} , i.e. 1350 W and 25.5 W (urban RN), in Tables 1.1 and 1.2, respectively, and the method in [65] for linearizing the total consumed power of various types of BS, we have obtained the following parameters regarding the abstracted power model of (1.81): $\Delta_{P,BS} = 7.5$, $P_{Ov,BS} = 375$ W as well as $P_{\max,BS} = 40$ W for the macro BS and $\Delta_{P,RN} = 6.3$, $P_{Ov,RN} = 6.45$ as well as $P_{\max,RN} = 1$ W such that $P_{BS} = 1350$ W and $P_{RN} = 25.5$ W for $t = 2$ as in Tables 1.1 and 1.2, respectively. In addition, we have set $P_{Ov,UE} = 100$ mW according to [69] and the ratio between transmission and reception overhead power as $\varsigma = 0.5$. Utilizing these parameter values, we have then compared the EE of MIMO AF against MIMO P2P in the in-building scenario in Figures 1.21 and 1.22. Notice that equations (1.78) and (1.82) revert to

$$C \approx \frac{1}{\ln(2)} \left[n \ln \left(\frac{\gamma_0}{d_0} \right) + r \left(\ln(1 + d_0) + \frac{1}{1 + d_0} - 1 \right) \right] \quad (1.84)$$

and

$$P_{\Sigma,P2P} = n(\Delta_{P,BS}P_1 + P_{Ov,BS}) + r\varsigma P_{Ov,UE}, \quad (1.85)$$

respectively, for MIMO P2P communication. In Figure 1.21, we plot the EE of MIMO P2P and MIMO AF as a function of the SNR offset between the direct and donor links, σ , for $n = q = 4$, $P_2 = 1$ W, $P_1 = 40$ W (P2P) and $P_1 = 37.3, 19.3$ and 1.3 W (AF) which have been obtained such that $P_{\Sigma,AF} = P_{\Sigma,P2P}$, $P_{\Sigma,AF} = 0.8P_{\Sigma,P2P}$ and $P_{\Sigma,AF} = 0.6P_{\Sigma,P2P}$, respectively. Assuming the same level of noise at the UE for both the P2P and AF cases, it implies that $\gamma_0 \in [0, 20]$ / $\gamma_1 = 15$ dB for P2P and $\gamma_0 \in [-0.3, 19.7]$ / $\gamma_1 = 14.7$ dB, $\gamma_0 \in [-3.1, 16.9]$ / $\gamma_1 = 11.9$ dB as well as $\gamma_0 \in [-14.8, 5.2]$ / $\gamma_1 = 0.2$ dB that corresponds to $P_1 = 37.3, 19.3$ and 1.3 W, respectively, for AF. Results first indicate that MIMO AF is far more energy efficient than P2P MIMO for the case of $r = 1$. Moreover, it can be remarked by comparing the blue with the red curves that MIMO AF can help to reduce the total consumed power while at the time slightly increasing the EE, which is most desirable. Indeed, EE being the ratio between SE and the total consumed power, it can be achieved either by increasing the SE while keeping the same P_{Σ} (or even if P_{Σ} increases) or reducing the total consumed power while keeping the same C (or even if C decreases). In the context of energy saving, the former approach for being energy efficient is the right one and these results indicate that MIMO AF can do just that. When reducing further $P_{\Sigma,AF}$ to $P_{\Sigma,AF} = 0.6P_{\Sigma,P2P}$, MIMO AF can still be more energy efficient than MIMO P2P when the quality of the donor link is at least 6 dB higher than the quality of the direct link. In the case that $r = 4$, MIMO AF can help to reduce the total consumed power by 20 % while being more energy efficient than MIMO P2P as long as $\sigma < -6$ dB.

In Figure 1.22, we depict the EE, SE and total consumed power of MIMO P2P as well as MIMO AF against the BS transmit power per antenna for various number of antennas and σ values. In addition, we consider that $n = q = 4$, $P_2 = 1$, γ_0 varies from -15 to 15 dB. In the left hand-side plot (EE plot), results first clearly show the existence of a maximum for the EE, which is not necessarily obtained for the maximum transmit power. Moreover, results confirm that MIMO AF EE gain over MIMO P2P increases as the number of receive antenna at the UE, r , decreases (when comparing the blue with the black curves) and as the quality of the donor link increases in comparison with the quality of the direct link (when comparing the brown, purple and blue dotted curves with the black dotted curve for $r = 1$). Looking now at the upper right-hand side graph (P_{Σ} plot), it shows that the total consumed power of the MIMO AF as a function of P_1 is always greater than that of MIMO P2P, which

is obvious due to the additional RN power consumption in MIMO AF. Thus, it implies that the better performances of MIMO AF against MIMO P2P in terms of EE (EE plot) are not due to power saving but SE improvement, as it is confirmed by the lower right-hand side graph (SE plot) where the SE gain of MIMO AF over MIMO P2P can be seen for different values of σ and $r = 1$. However, one can also look at these graphs in a different way. Let us assume that we want to use MIMO AF to reduce the total consumed power by 20 % in comparison with MIMO P2P when $\sigma = 0$ dB and $r = 1$. It corresponds in the x-axis of the P_Σ plot to a reduction of 5 dBm in the BS transmit power per antenna, which in turn corresponds to an increase of 50 % for the EE (see EE plot). As a reminder of the existence of a trade-off between EE and SE [70], this power saving will come at the cost of a 3 bits/s/Hz reduction (see SE plot).

Overall, the results reveals that relaying can increase the EE in comparison with P2P communication by either power saving or SE improvement in an in-building scenario, especially when the number of receive antennas at the UE is lower than the number of antennas at the BS and RN as well as when the quality of the donor link is higher than the quality of the direct link. Results also indicate that even though transmitting with maximum power implies maximum SE, it does not necessarily imply maximum EE.

1.5 Conclusion and Future Works

In this chapter, a comprehensive investigation of cooperative communication systems has been presented and fundamental understanding from both the theoretical and practical points of view has been achieved. We considered typical relaying schemes including AF, DF CF, and hybrid schemes and studied their spectral and energy efficiency performances at both link and system levels.

Flexible approaches have been taken to combine different forwarding strategies, enabling the system to efficiently and dynamically adapt itself to the variations of the channel. The CF/DF based strategy shows significant improvement in terms of throughput and energy consumption. However, it should be emphasized that compared with direct transmission,

the cooperative strategy only shows improved energy efficiency when the distance between the destination and the source is large. The main advantage of the proposed hybrid CF/DF or AF/DF based strategy is that it can achieve either transmit or receive diversity. Another issue we need to emphasize is the power model employed. For a meaningful analysis we need to strike the right balance between realistic modelling and mathematical tractability and we believe that the very important aspect of realistic energy consumption is well captured by our current power model.

Furthermore, relay has been studied in cellular networks. We have used more complex and realistic models for the BS and RN. Analysis shown that RNs should be deployed at the cell edge to improve the energy efficiency. The number of RNs deployed in a sector should be optimized in terms of energy consumption. Deploying more RNs in a sector might be able to improve the average capacity of the system, but it also causes more energy consumption. When the disadvantage it brings outweighs the benefit, using more RN provides little spectrum improvement but occurs huge energy consumption, leading to low EE. Generally speaking, we can reach the conclusion that green communication is able to benefit from the usage of relaying technology with delicate design.

Although our work has significantly contributed towards the improvement of cooperative communication systems both in terms of SE and EE, there are still numerous opportunities for further improvements. In multiple RN case, using coordinated multi-point Tx/Rx of RNs might be more efficient than relay selection and, thus, it is an interesting topic to investigate. The current relay architectures, which are defined in IEEE 802.16m and 3GPP LTE-Advanced, are only optimized for fixed relay, i.e. the RN is attached to a designated BS and becomes a part of the fixed access network. A mobile relay architecture, where relay can change their BS attachment according to operation demand, will promise more resilient and flexible relay deployment. Furthermore, network coding for the two-way relay channel is also regarded as one of the key enabling techniques for green communication.

References

- [1] Ericsson Review, "HSDPA Performance and Evolution," no. 03, Mar. 2006.
- [2] Ericsson White Paper, "Long Term Evolution (LTE): an introduction," Oct. 2007.
- [3] Sesia, Toufik, Baker, *LTE - The UMTS Long Term Evolution: From Theory to Practice*, Wiley, 2009
- [4] WiMax Forum at <http://www.wimaxforum.org/>.
- [5] Press release, *EU Commissioner Calls on ICT Industry to Reduce Its Carbon Footprint by 20% as Early as 2015*, MEMO/09/140, Mar. 2009.
- [6] *Vodafone Corporate Responsibility Report*, 2008.
- [7] <http://fireworks.intranet.gr/>
- [8] <http://www.ict-rocket.eu/>
- [9] I. Stanojev, O. Simeone, Y. Bar-Ness, and D. Kim, "Energy efficiency of non-collaborative and collaborative hybrid-ARQ protocols," *IEEE Trans. Wireless Commun.*, vol. 8, no. 1, pp. 326-335, Jan. 2009.
- [10] Yinan Qi, Reza Hoshyar, Imran Ali Muhammad, and Rahim Tafazolli, "Energy Efficiency Analysis of Hybrid-ARQ in Hybrid Relaying Systems," in *Proc. of VTC 2011*.
- [11] Madan, R., Mehta, N., Molisch, A., and Jin Zhang, "Energy-Efficient Cooperative Relaying over Fading Channels with Simple Relay Selection," *IEEE Trans. Wireless Commun.*, vol. 7, no. 8, pp. 3013-3025, Aug. 2008.
- [12] Yinan Qi, Reza Hoshyar, Muhammad Ali Imran, and Rahim Tafazolli, "H²-ARQ-Relaying: Spectrum and Energy Efficiency Perspectives," *IEEE Journal on Selected Areas in Communications*, vol. 29, no. 8, pp. 1547-1558, Sep. 2011.
- [13] <http://www.ict-earth.eu/>
- [14] E.C. van der Meulen, "Three-terminal Communication Channel," *Adv. Appl. Prob.*, vol. 3, pp. 120-154, 1971.
- [15] Cover. T, and Gamal. A.E., "Capacity Theorems for the Relay Channel," *IEEE Trans. Inform. Theory*, vol. 25, pp. 572-584, Sep. 1979.
- [16] R. U. Nabar, H. Bolcskei and F.W. Kneubuhler, "Fading relay channels: performance limits and space-time signal design," *IEEE J. Sel. Area. in Comm.*, Aug 2004.
- [17] L. Zhao and Z. Liao, "Power Allocation for Amplify-and-Forward Cooperative Transmission Over Rayleigh-Fading Channels", *Journal of Communications*, pp. 33-42, vol.

- 3, No. 3, July. 2008.
- [18] M. Yu and J. Li, "Is Amplify-and-forward Practically Better Than Decode-and-forward or Vice Versa?" in *Proc. IEEE Int. Conf. Acoustics, Speech, and Signal Processing (ICASSP)*, vol. 3, March 2005, pp. 365-368.
- [19] M. R. Souryal and B. R. Vojcic, "Performance of Amplify-and-forward and Decode-and-forward Relaying in Rayleigh Fading with Turbo Codes", *Int. Conf. Acoustics, Speech, and Signal Processing (ICASSP)*, vol. 4, May 2006, pp. 681-684.
- [20] Janani, M., Hedayat, A., Hunter, T.E. and Nosratinia, A. "Coded cooperation in wireless communications: space-time transmission and iterative decoding," *IEEE Trans. Signal Processing*, vol. 52, pp 362-371, Feb. 2004.
- [21] Hunter, T.E. and Nosratinia, A. "Diversity through coded cooperation," *IEEE Trans. Wireless Commun.*, vol. 5, pp. 283-289, Feb, 2006.
- [22] Zhihan Yi and Min Kim, "Diversity order analysis of the decode-and-forward cooperative networks with relay selection," *IEEE Trans. Wireless Commun.*, vol. 7, no. 5, pp. 1792-1799, May, 2008.
- [23] T. Q. Duong and V. N. Q. Bao, "Performance analysis of selection decode-and-forward relay networks," *IEE Electronics Letters*, vol. 44, pp. 1206-1207, Sep. 2008.
- [24] Christos K. Datsikas, Nikos C. Sagias, Fotis I. Lazarakis, and George S. Tombras, "Outage analysis of decode-and-forward relaying over nakagami-m fading channels," *IEEE Signal Processing Letters*, vol. 15, pp. 41-44, 2008.
- [25] J. N. Laneman, *Cooperative diversity in wireless networks: Algorithms and architectures*, PhD thesis, Massachusetts Institute of Technology, 2002
- [26] Peyman Razaghi and Wei Yu, "Bilayer Low-Density Parity-Check Codes for Decode-and-Forward in Relay Channels," *IEEE Trans. Inform. Theory*, vol. 53, no. 10, pp. 3723-3739, Oct. 2007.
- [27] J.N.Laneman, D.N.C. Tse, G.W. Wonell, "Cooperative diversity in wireless networks: Efficient protocols and outage behavior", *IEEE Trans. Inform. Theory*, vol. 50, no. 12, pp. 3062-3080, Dec. 2004.
- [28] A. Host-Madsen and J. Zhang, "Capacity bounds and power allocation for wireless relay channels," *IEEE Trans. Inform. Theory*, vol. 51, pp. 2020 - 2040, Jun 2005.
- [29] Michael Kats and Shlomo Shamai, "Relay Protocols for Two Colocated Users," *IEEE*

- Trans. Inform. Theory*, vol. 52, No. 6, pp. 2329-2344, Jun. 2006.
- [30] Zhixin Liu, Vladimir and Zixiang Xiong, "Wyner-Ziv Coding for the Half-duplex Relay Channel," *IEEE Conference on Acoustics, Speech and Signal Processing*, vol.5, pp. 1113-1116, Mar. 2005
- [31] Ruiyuan Hu and Jing Li, "Practical Compress-Forward in User Cooperation: Wyner-Ziv Cooperation," *IEEE International Symposium on Information Theory*, Jul. 2006.
- [32] Yonghui Li, B. Vucetic, Zhuo Chen, and Jinhong Yuan, "An improved relay selection scheme with hybrid relaying protocols," in *Proc. IEEE Global Telecommunications Conf. (GLOBECOM'07)*, pp. 3704-3708, New Orleans, USA, Nov. 2007.
- [33] Yonghui Li, B. Vucetic, and Jinhong Yuan, "Distributed turbo coding with hybrid relaying protocols," in *Proc. IEEE 19th Int. Symp. on Personal, Indoor and Mobile Radio Communications (PIMRC'08)*, pp. 1-6, Cannes, France, Sept. 2008.
- [34] S. Serbetli and A. Yener, "Power allocation and hybrid relaying strategies for F/TDMA Ad Hoc networks," in *Proc. IEEE Int. Conf. on Commun.(ICC'06)*, vol. 4, pp. 1562-1567, Istanbul, Turkey, Jun. 2006.
- [35] 3GPP TR 36.814 v1.5.1(2009-12), *Further Advancement for E-UTRA, Physical Layer Aspects*.
- [36] IEEE Std 802.16j at <http://ieee802.org/16/pubs/80216j.html>
- [37] IEEE Std 802.16m at <http://ieee802.org/16/tgm/>
- [38] Ericsson Research White Paper "LTE-Advanced : Evolving LTE towards IMT-Advanced," 2010.
- [39] EARTH deliverable, "Most Promising Tracks of Green Network Technologies" 2011, at <https://www.ict-earth.eu/publications/deliverables/deliverables.html>.
- [40] Yinan Qi, Reza Hoshyar, and Rahim Tafazolli, "A Novel Hybrid Relaying Scheme Using Multilevel Coding," in *Proc. of VTC-2010 Spring*, 2010, pp. 1-5.
- [41] S. Cui, A. J. Goldsmith and A. Bahai, "Energy-Constrained Modulation Optimization", *IEEE Trans. Wireless Commun.*, vol. 4, no. 5, pp. 2349-2360, Sep. 2005.
- [42] Yinan Qi *Single Relay Cooperative Transmission/Reception Techniques*, PhD thesis, University of Surrey, 2009.
- [43] A. Wyner and J. Ziv, "The Rate-distortion Function for Source Coding with Side Information at the Decoder," *IEEE Trans. Inform. Theory*, vol. 22, pp. 1-10, Jan. 1976.

- [44] A. Wyner, "The rate-distortion function for source coding with side information at the decoder-ii: General sources," *Inf. Control*, vol. 38, pp. 60-80, 1978.
- [45] D. Slepian and J. K. Wolf, "Noiseless coding of correlated information sources," *IEEE Trans. Inform. Theory*, vol. 19, pp. 471-480, July 1973.
- [46] Sergio D. Servetto, "Lattice quantization with side information," in *Proc. Data Compression Conf. (DCC'03)*, Snowbird, UT, Mar. 2003, pp. 510-519.
- [47] Ram Zamir and Shlomo Shamai, "Nested linear / lattice codes for Wyner-Ziv Encoding," in *Proc. Information Theory Workshop (ITW)*, Killarney, Ireland, Jun. 1998, pp. 92-93.
- [48] Zhixin Liu, Cheng, S., Liveris, A.D. and Zixiang Xiong, "Slepian-Wolf Coded Nested Lattice Quantization for Wyner-Ziv Coding: High-Rate Performance Analysis and Code Design," *IEEE Trans. Inform. Theory*, vol.52, pp. 4358-4379, Oct. 2006.
- [49] K. Singhal, J. Vlach, and M. Vlach, "Numerical inversion of multidimensional Laplace transform," in *Proc. of the IEEE*, vol. 63, no. 11, pp. 1627 - 1628, Nov. 1975.
- [50] Larry L. Peterson and Bruce S. Davie, *Computer Networks: A Systems Approach*, Third Edition, London, Academic Press, 2003.
- [51] S. Kallel and D. Haccoun, "Sequential decoding with ARQ and code combining: a robust hybrid FEC/ARQ system," *IEEE Trans. Commun.*, vol. 36, no. 7, pp. 773-780, Jul. 1988.
- [52] D. N. Rowitch and L. B. Milstein, "On the performance of hybrid FEC/ARQ systems using rate compatible punctured turbo (RCPT) codes," *IEEE Trans. Commun.*, vol. 48, no. 6, pp. 948-959, Jun. 2000.
- [53] F. Babich, G. Montorsi, and F. Vatta, "Some notes on rate-compatible punctured turbo codes (RCPTC) design," *IEEE Trans. Commun.*, vol. 52, no. 5, pp. 681-684, May 2004.
- [54] J. Hagenauer, "Rate-compatible punctured convolutional codes (RCPC Codes) and their applications," *IEEE Trans. Commun.*, vol. 36, no. 4, pp. 389-400, Apr. 1988.
- [55] S. Kallel and D. Haccoun, "Generalized type-II hybrid ARQ scheme using punctured convolutional coding," *IEEE Trans. Commun.*, vol. 38, no. 11, pp. 1938-1946, Nov. 1990.
- [56] Giuseppe Caire and Daniela Tuninetti, "The Throughput of Hybrid-ARQ Protocols for the Gaussian Collision Channel," *IEEE Trans. Inform. Theory*, vol. 47, No. 5, pp.

- 1971-1988, Jul. 2001.
- [57] Wang Rui, Lau, V.K.N., "Combined cross-layer design and HARQ for multiuser systems with outdated channel state information at transmitter (CSIT) in slow fading channels," *IEEE Trans. Wireless Commun.*, vol. 7, pp. 2771-2777, Jul. 2008.
- [58] Tabet, T., Dusad, S., and Knopp, R., "Diversity-Multiplexing-Delay Tradeoff in Half-Duplex ARQ Relay Channels," *IEEE Transactions on Inform. Theory*, vol. 53, no. 10, pp. 3797 - 3805, Oct. 2007.
- [59] Lin Dai and Letaief, K., "Throughput maximization of ad-hoc wireless networks using adaptive cooperative diversity and truncated ARQ," *IEEE Transactions on Communications*, vol. 56, no. 11, pp. 1907-1918, Nov. 2008.
- [60] Bin Zhao and Valenti, M.C., "Practical relay networks: a generalization of hybrid-ARQ," *IEEE Journal on Selected Areas in Communications (JSAC)*, vol. 23, no.1, pp. 7-18, Jan. 2005.
- [61] M.N. Khormuji and E. G. Larsson, "Analytical Results on Block Length Optimization for Decode-and-forward Relaying with CSI Feedback," in *Proc. 8th IEEE Workshop on Signal Processing Advances in Wireless Communications*, June 2007, Helsinki, Finland
- [62] S. Igor, S. Osvaldo, B. Yeheskel and Cho Myeon Yun, "On the Optimal Number of Hops in Linear Wireless Ad-Hoc Networks with Hybrid ARQ," in *Proc. of WiOPT*, Apr. 2008.
- [63] R. Hoshyar, and R. Tafazolli, "Performance evaluation of HARQ schemes for cooperative regenerative relaying," in *Proc. of IEEE Int. Conf. on Commun.(ICC'09)*, Dresden, Germany, Jun. 2009.
- [64] Technical Specification Group Radio Access Network, "Evolved universal terrestrial radio access (EUTRA); LTE radio frequency (RF) system scenarios," 3rd Generation Partnership Project (3GPP), Tech. Rep. TS 36.942, 2008-2009.
- [65] G. Auer et al., "D2.3: Energy Efficiency Analysis of the Reference Systems, Areas of Improvements and Target Breakdown," INFISO-ICT-247733 EARTH (Energy Aware Radio and NeTwork TecHnologies), Tech. Rep., Nov. 2010.
- [66] EARTH deliverable 3.2 online at <https://www.ict-earth.eu/publications/deliverables/deliverables.html>.
- [67] J. Wagner, B. Rankov, and A. Wittneben, "Large N Analysis of Amplify-and-Forward

- MIMO Relay Channels with Correlated Rayleigh Fading,” *IEEE Trans. Inf. Theory*, vol. 54, no. 12, pp. 5735–5746, Dec. 2008.
- [68] F. Hélot, M. A. Imran, and R. Tafazolli, “Energy Efficiency Analysis of In-Building MIMO AF Communication,” in *Proc. IWCMC 2011*, Istanbul, Turkey, Jul. 2011.
- [69] G. Miao, N. Himayat, and G. Y. Li, “Energy-Efficient Link Adaptation in Frequency-Selective Channels,” *IEEE Trans. Commun.*, vol. 58, no. 2, pp. 545–554, Feb. 2010.
- [70] S. Verdu, “Spectral Efficiency in the Wideband Regime,” *IEEE Trans. Inf. Theory*, vol. 48, no. 6, pp. 1319–1343, Jun. 2002.

Table 1.1: Macro BS Power Model

| Macro | | | |
|--------------------------|-------------------------|-------|--------|
| PA | Max Transmit rms power | [dBm] | 46.0 |
| | Max Transmit rms power | [W] | 39.8 |
| | PAPR | [dB] | 8.0 |
| | Peak Output Power | [dBm] | 54.0 |
| | Pdc | [W] | 128.2 |
| | Power-Added Efficiency | [%] | 31.1 |
| TRX | Max Transmit rms power | [dBm] | -8.0 |
| | TX Pdc | [W] | 6.8 |
| | RX Pdc | [W] | 6.1 |
| | Total Pdc | [W] | 13.0 |
| BB | Radio[inner rx/tx] | [W] | 10.8 |
| | LTE turbo [outer rx/tx] | [W] | 8.8 |
| | Processors | [W] | 10.0 |
| | Total Pdc | [W] | 29.5 |
| DC-DC | loss | [%] | 8.0 |
| | Pdc | [W] | 13.7 |
| Cooling | loss | [%] | 12.0 |
| | Pdc | [W] | 22.1 |
| Main Supply | loss | [%] | 9.0 |
| | Pdc | [W] | 18.6 |
| Total 1 Radio | | [W] | 225.0 |
| Number of Sectors | | # | 3.0 |
| Number of PAs | | # | 2.0 |
| Total N Radio | | [W] | 1350.0 |

Table 1.2: RN Power Model

| RN | | | | |
|----------------------|-------------------------|-------|--------------|--------------|
| | | | Rural | Urban |
| PA | Max Transmit rms power | [dBm] | 37.0 | 30.0 |
| | Max Transmit rms power | [W] | 5.0 | 1.0 |
| | PAPR | [dB] | 8.0 | 12.0 |
| | Peak Output Power | [dBm] | 45.0 | 42.0 |
| | Pdc | [W] | 14.1 | 2.8 |
| | Power-Added Efficiency | [%] | 35.6 | 35.6 |
| TRX | Max Transmit rms power | [dBm] | -14.0 | -21.0 |
| | TX Pdc | [W] | 1.6 | 0.6 |
| | RX Pdc | [W] | 2.2 | 0.9 |
| | Total Pdc | [W] | 3.8 | 1.5 |
| BB | Radio[inner rx/tx] | [W] | 2.3 | 2.3 |
| | LTE turbo [outer rx/tx] | [W] | 2.0 | 2.0 |
| | Processors | [W] | 2.5 | 2.5 |
| | Total Pdc | [W] | 6.8 | 6.8 |
| DC-DC | loss | [%] | 6.4 | 6.4 |
| | Pdc | [W] | 1.6 | 0.7 |
| Cooling | loss | [%] | 0.0 | 0.0 |
| | Pdc | [W] | 0.0 | 0.0 |
| Main Supply | loss | [%] | 7.7 | 7.7 |
| | Pdc | [W] | 2.0 | 0.9 |
| Total 1 Radio | | [W] | 28.3 | 12.8 |
| Number of PAs | | # | 2.0 | 2.0 |
| Total N Radio | | [W] | 56.5 | 25.5 |

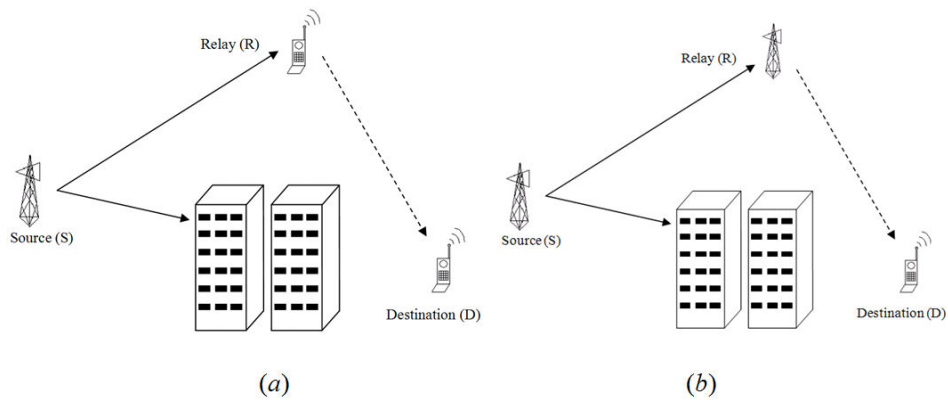


Figure 1.1: A relay system in the urban environment. (a) mobile relay (b) fixed relay

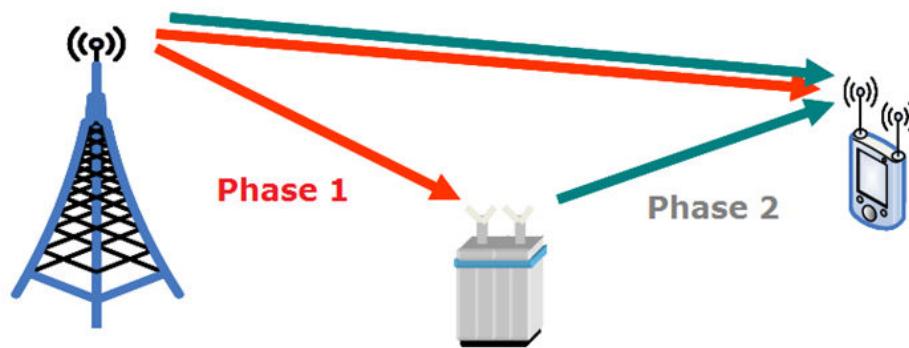


Figure 1.2: Half-duplex Relaying.

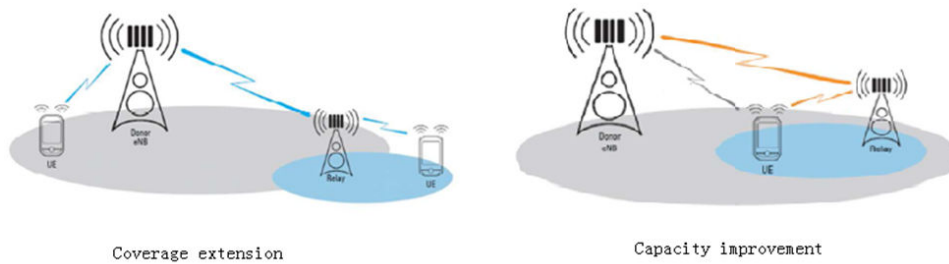


Figure 1.3: Relay deployment approaches.

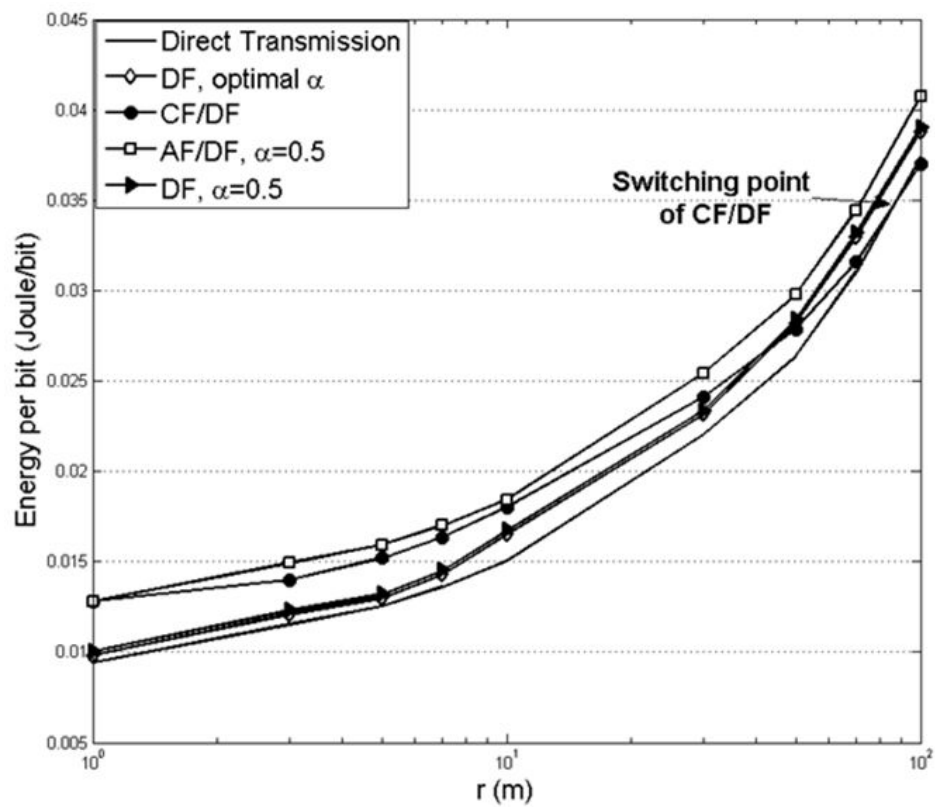


Figure 1.4: Energy per bit in shot range.

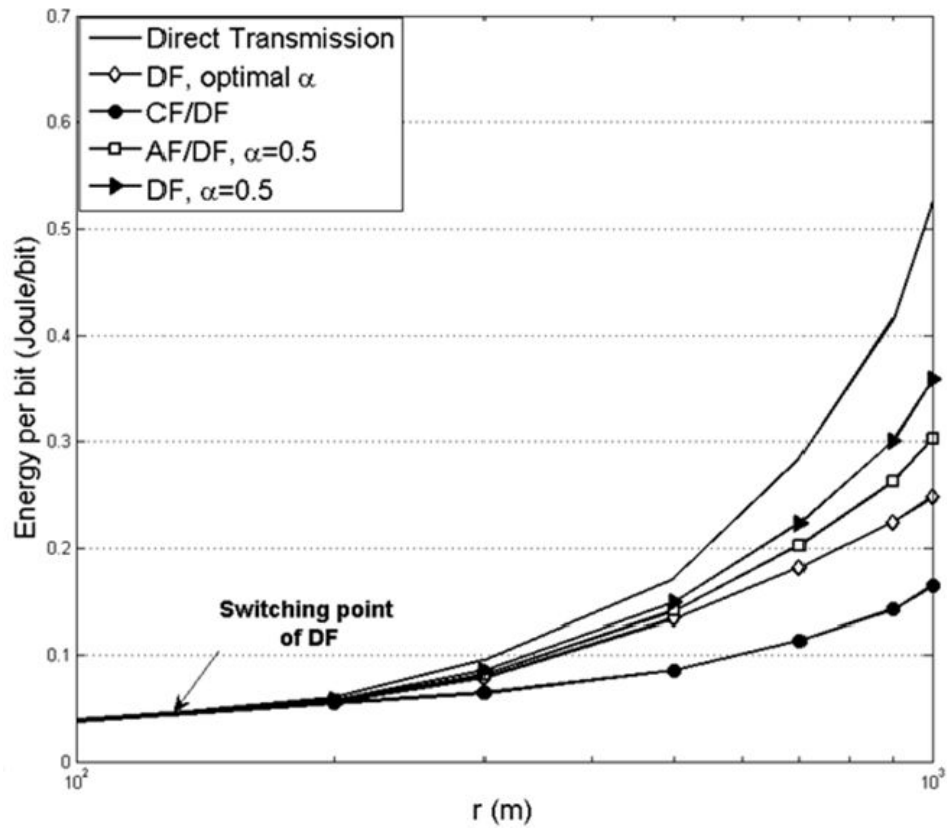


Figure 1.5: Energy per bit in long range.

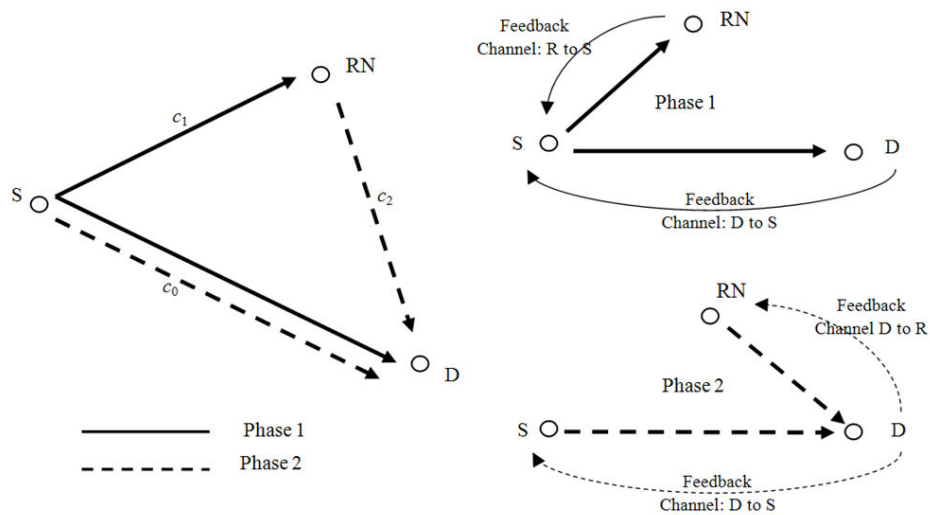


Figure 1.6: Feedback Channel.

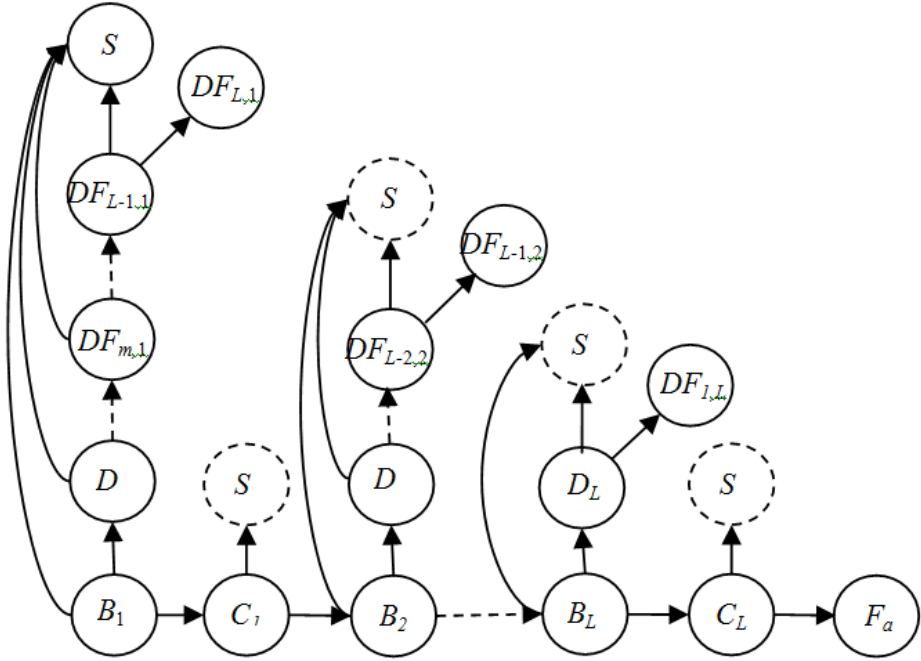


Figure 1.7: State Diagram.

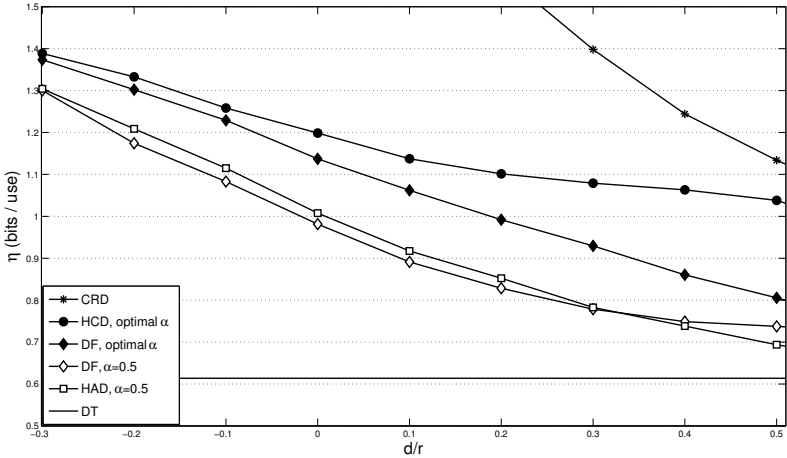


Figure 1.8: Spectrum Efficiency.

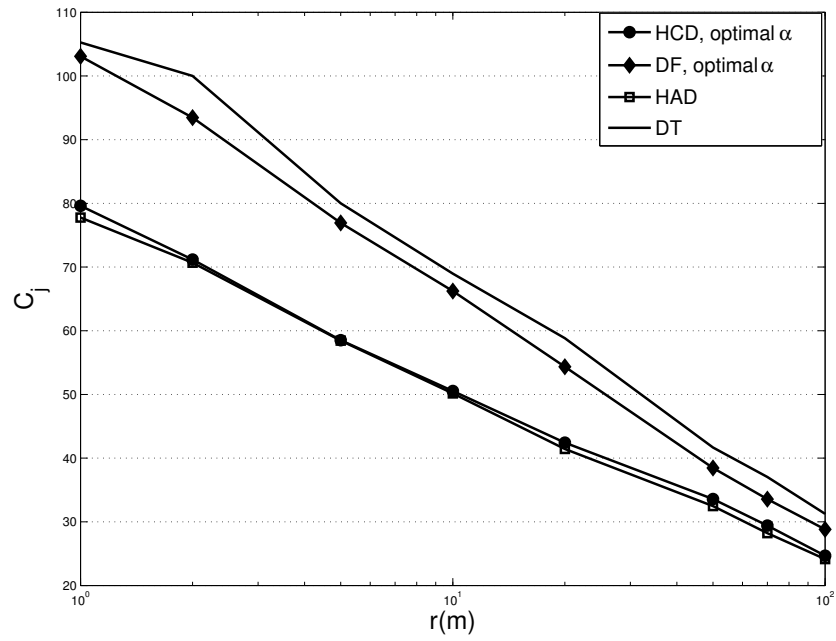


Figure 1.9: Energy Efficiency in Short Distance.

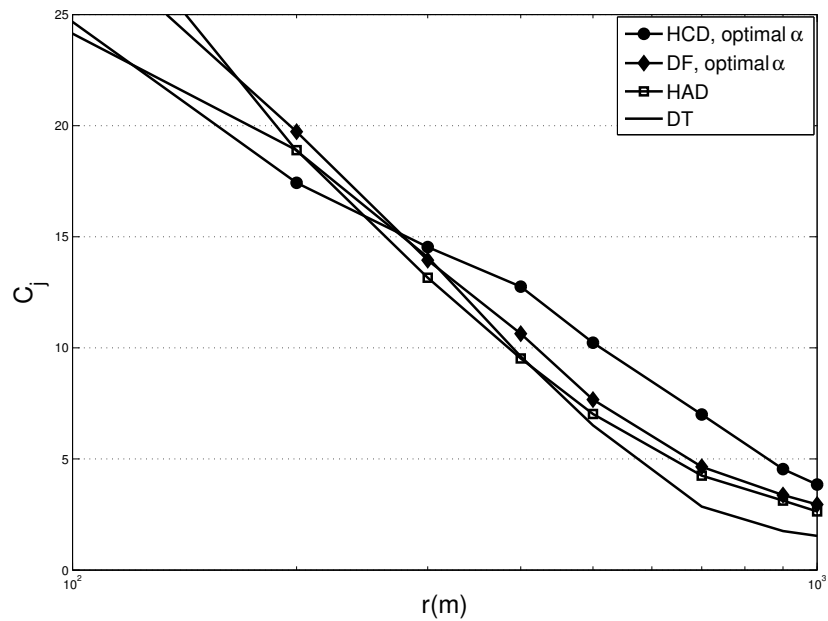


Figure 1.10: Energy Efficiency in Long Distance.

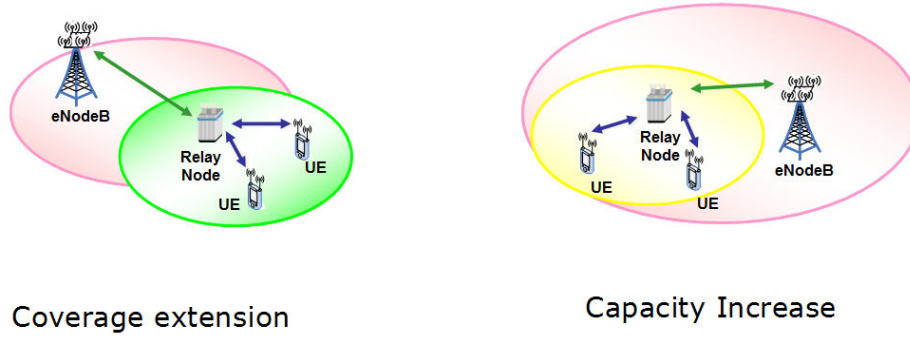


Figure 1.11: RNs in cellular networks.

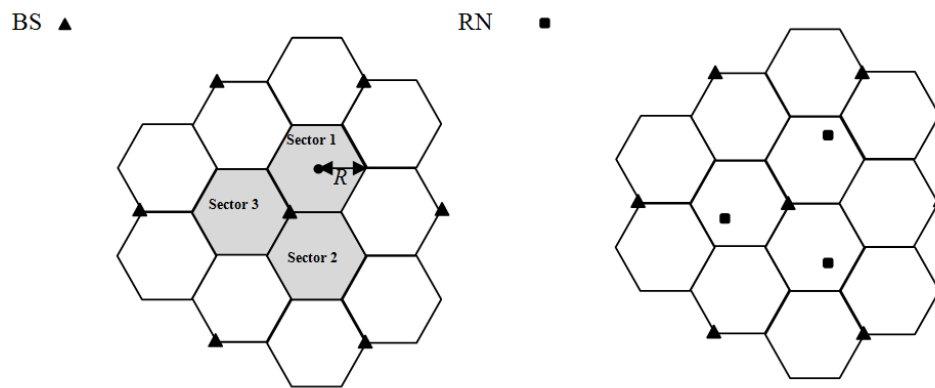


Figure 1.12: Cellular System.

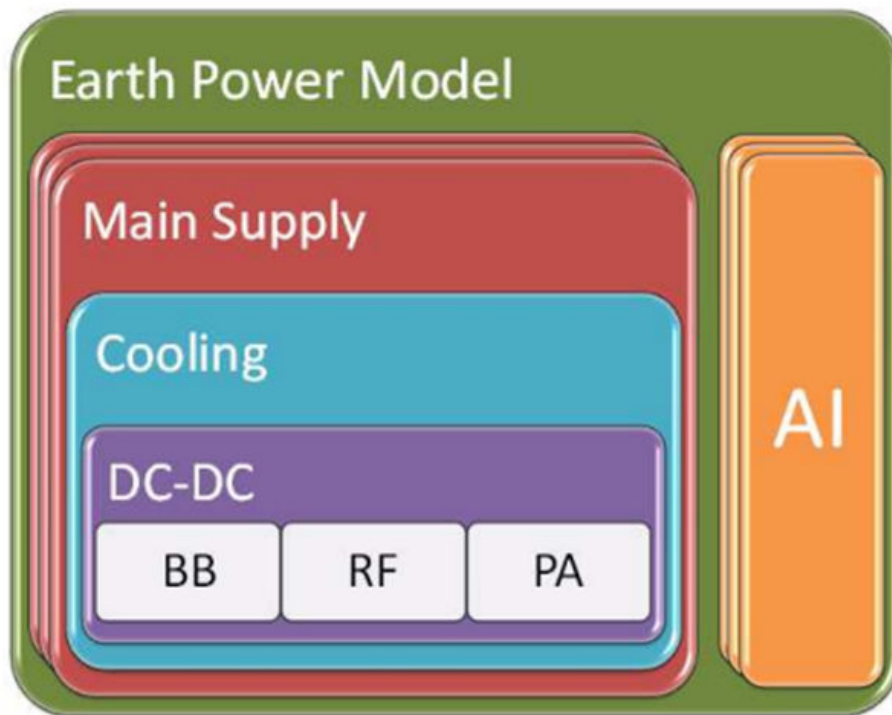


Figure 1.13: Power Model.

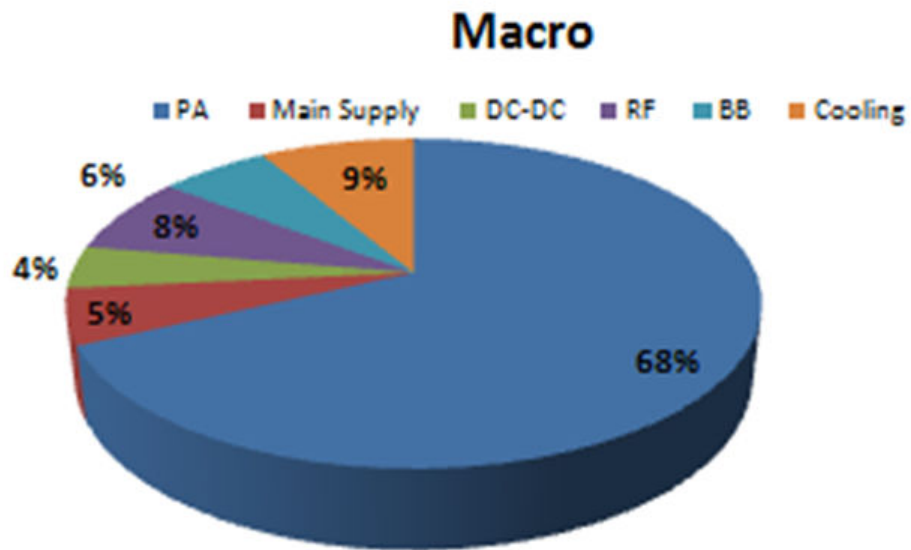


Figure 1.14: Macro Power Model Breakdown.

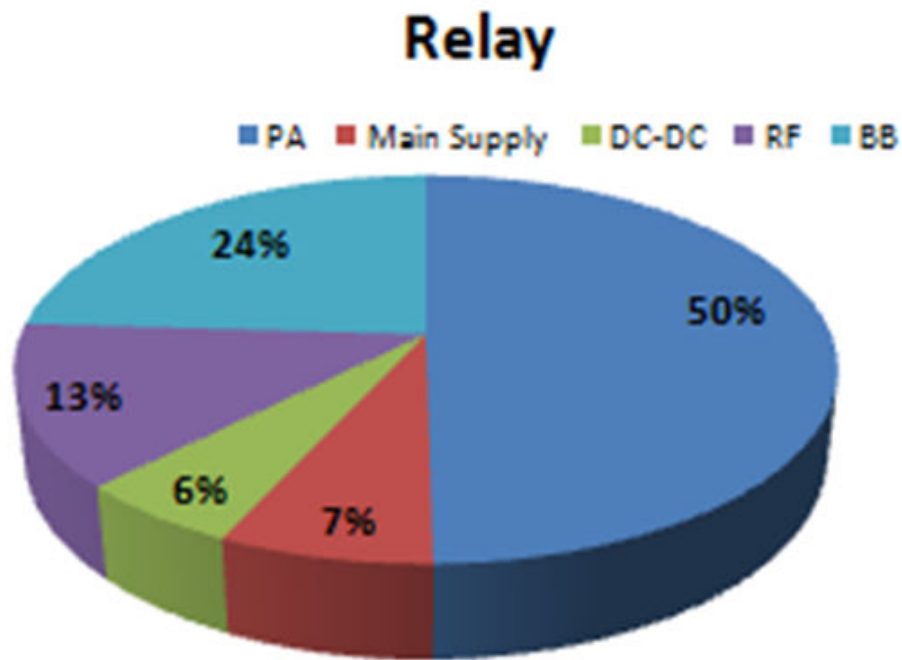


Figure 1.15: RN Power Model Breakdown.

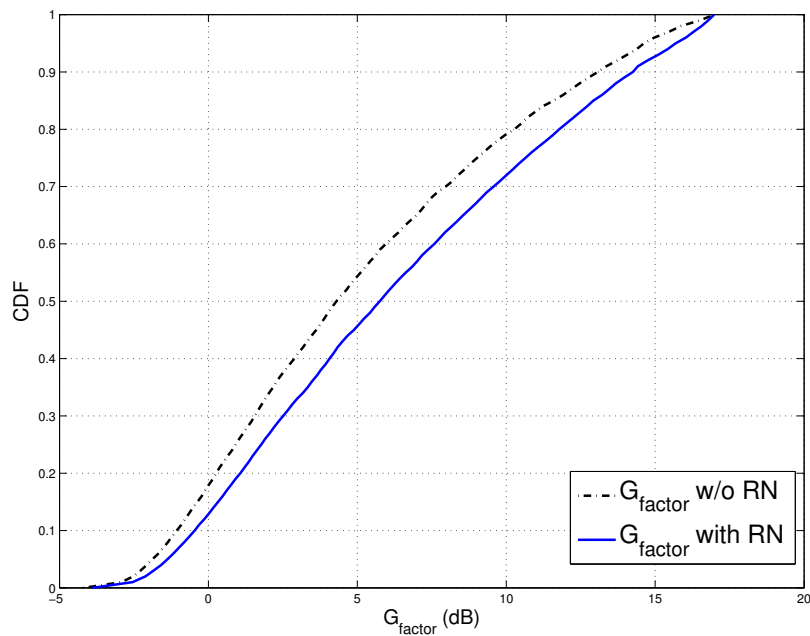


Figure 1.16: CDF of $G_{fac,eq}$

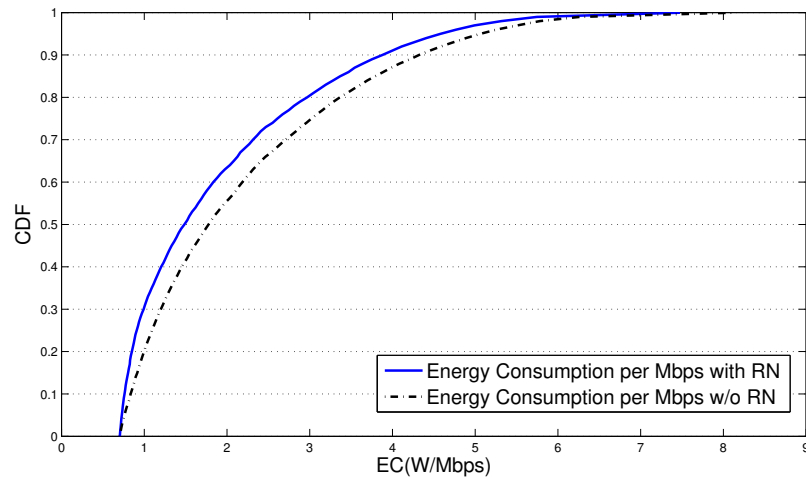


Figure 1.17: CDF of Energy Consumption per Mbps.

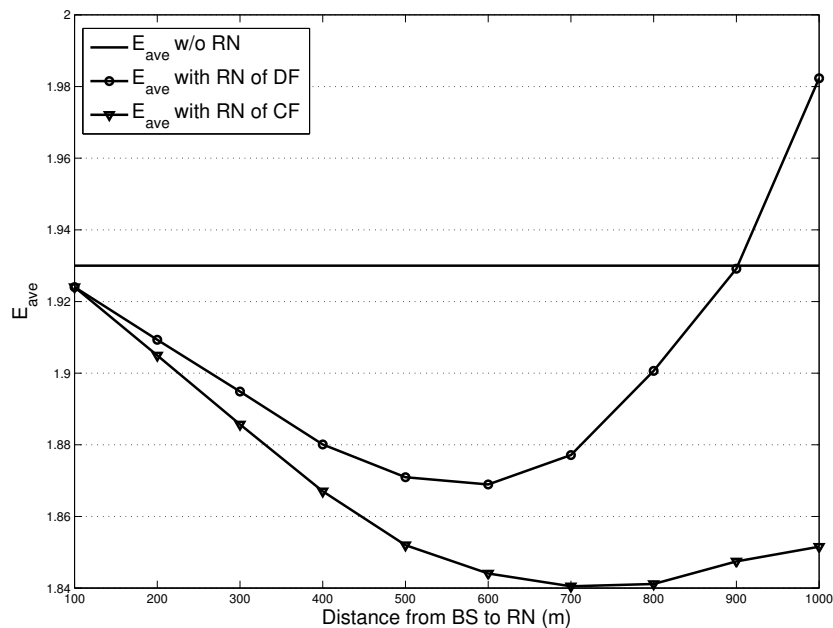


Figure 1.18: E_{ave} with Single RN

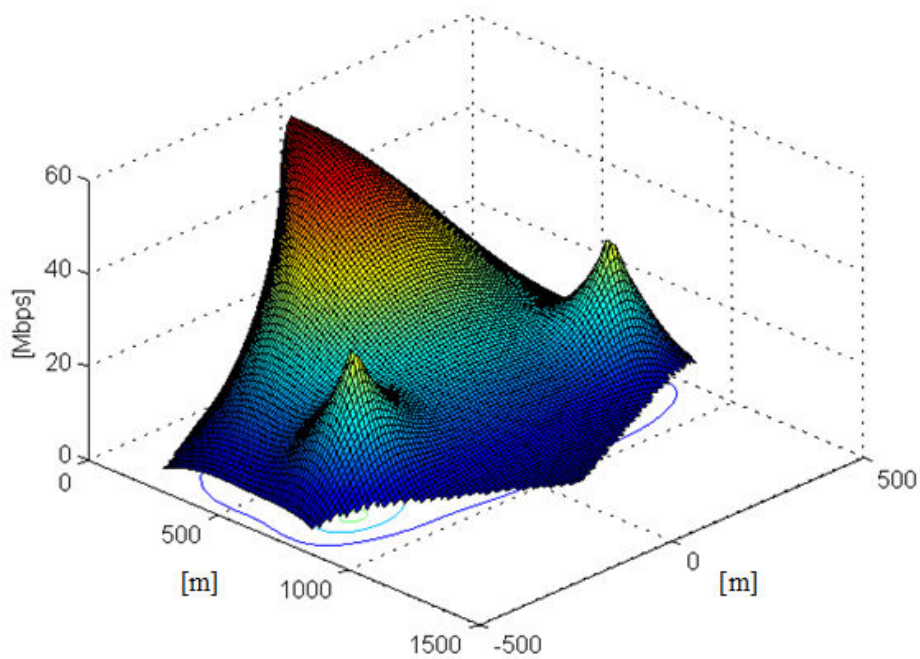
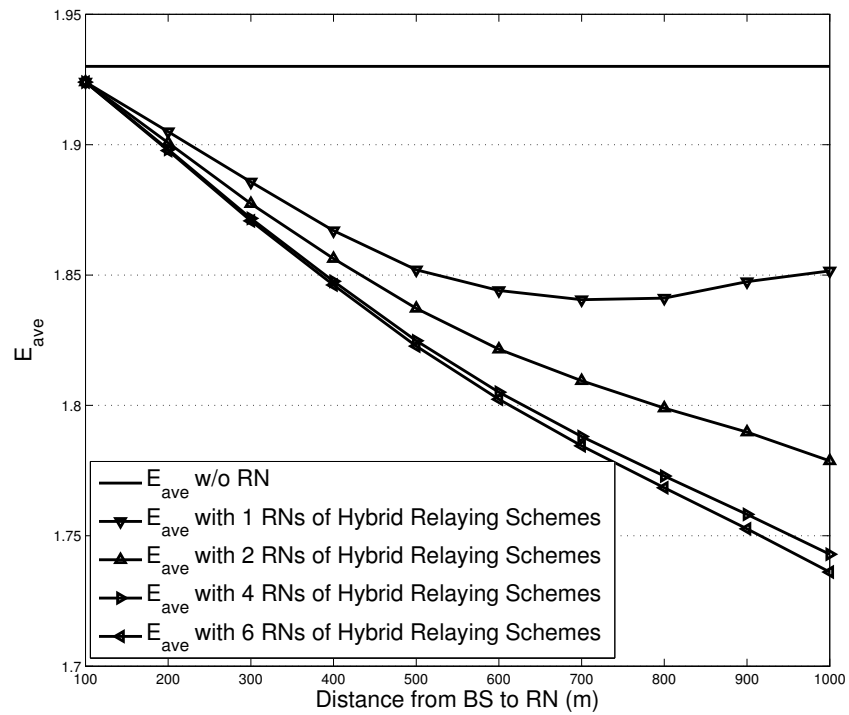


Figure 1.19: Capacity with Two RNs.

Figure 1.20: E_{ave} with Multiple RNs

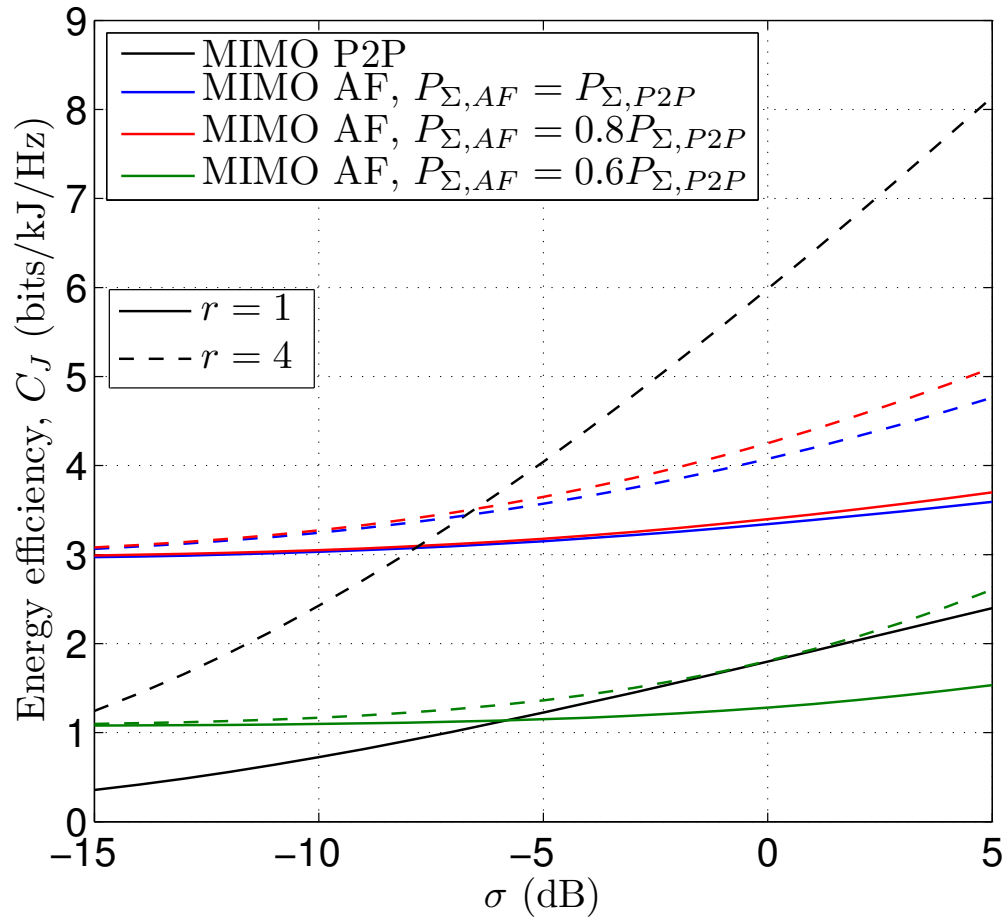


Figure 1.21: EE of MIMO P2P and MIMO AF as a function the SNR offset between the donor and direct links for $n = q = 4$.

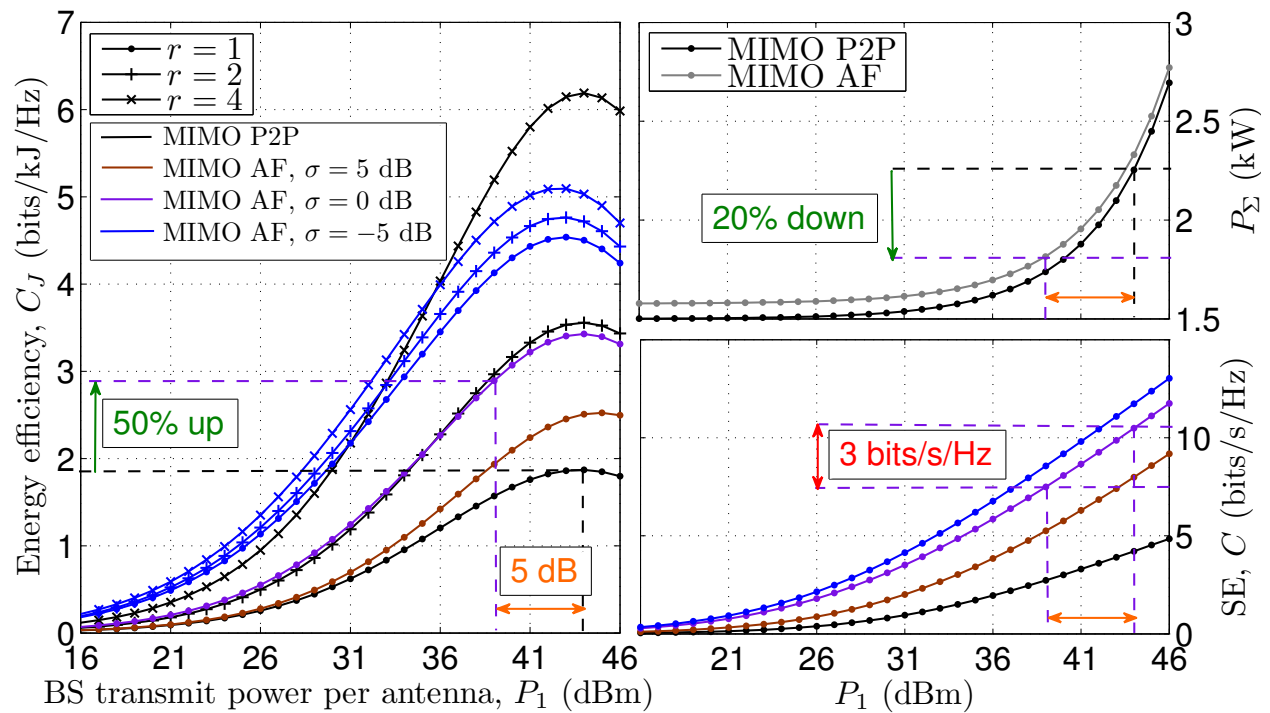


Figure 1.22: EE, SE and total consumed power of MIMO P2P as well as MIMO AF vs. the BS transmit power per antenna in dBm for various number of antennas and σ values.